



**1 Identification of erosion hotspots and scale-dependent runoff controls on
2 sediment transport in an agricultural catchment**

3 Christopher Thoma^{1,2}, Borbala Szeles^{1,2}, Miriam Bertola^{1,2}, Elmar M. Schmaltz³, Carmen
4 Krammer³, Peter Strauss³, Günter Blöschl^{1,2}

5 ¹ Institute of Hydraulic Engineering and Water Resources Management, Vienna University of
6 Technology, Vienna, Austria

7 ² Centre for Water Resource Systems, Vienna University of Technology, Vienna, Austria

8 ³ Institute for Land and Water Management Research, Federal Agency for Water
9 Management, Petzenkirchen, Austria

10 **Corresponding author:** Christopher Thoma

11 **E-mail address:** thoma@hydro.tuwien.ac.at

12

13 **Abstract:**

14 Understanding how agricultural land management influences sediment transport is crucial for
15 identifying critical source areas (CSAs) and improving erosion mitigation strategies. While
16 numerous studies focus on in-stream sediment concentrations, fewer investigate overland
17 flow on the hillslopes. We monitored streamflow and sediment fluxes at an overland flow
18 station (E2) and an in-stream station (MW) across 55 runoff events (2012–2022) in the
19 Hydrological Open Air Laboratory (HOAL), Austria. The catchment was segmented into four
20 distinct areas (A, B, GW9, C) based on topography, hydrological connectivity, and proximity to
21 the stream, allowing a spatially explicit assessment of erosion hotspots. Temporal patterns of
22 sediment transport were analysed to infer spatial variability, and differences in sediment
23 transport dynamics among areas were quantified using Kruskal-Wallis tests and effect size
24 analysis. Results suggest that at E2 (hillslope scale), non-erosive cultivation significantly
25 reduced peak turbidity (~9.5 times) and sediment load (~3.8 times) in flat agricultural areas
26 (7.2% slope, <500 m from the stream) but had no measurable effect in steep (10–12% slope)
27 or distant (>1000 m) agricultural areas. Across all field types, conversion to non-erosive
28 cultivation did not affect peak flow. At MW (catchment scale), compared to E2, peak turbidity
29 at MW decreased (~5.4–7.7 times) due to dilution from subsurface flow contributions, while
30 peak flow increased (~2.8–11 times) due to additional inputs from wetlands, springs, and
31 subsurface flows. Sediment load at MW was ~2.4–5.4 times higher than at E2, likely due to
32 unmonitored diffuse overland flow and sediment inputs from tile drainages. Our findings
33 indicate that non-erosive cultivation alone in steep terrains or distant agricultural areas is
34 insufficient to effectively mitigate sediment transport. Effective sediment management in
35 agricultural catchments requires spatially targeted erosion control strategies that account for
36 topography, hydrological connectivity, and field proximity to streams.

37

38

39



1. Introduction

The loss of topsoil due to erosion leads to decreased soil fertility, reduced organic matter content, and diminished water retention capacity, ultimately impairing agricultural productivity and food security (Borrelli et al., 2020; FAO, 2020). Beyond agricultural losses, sediment transport into water bodies introduces nutrient imbalances, particularly phosphorus and nitrogen, which drive eutrophication and harmful algal blooms, degrading freshwater resources (Akinawo, 2023).

Agricultural catchments are particularly vulnerable to erosion during intense rainfall events, where overland flow mobilizes soil from cultivated fields (Firoozi and Firoozi, 2024). The magnitude of sediment transport depends on natural drivers—including precipitation intensity, soil moisture, and slope (Nearing et al., 2017; Kirkby et al., 2000; Fryirs, 2013)—as well as anthropogenic influences, such as tillage intensity and cropping systems (Boardman and Poesen, 2006; Lal, 2015). While natural erosion drivers cannot be controlled, targeted land management strategies can significantly reduce sediment transport to streams (Tomer and Schilling, 2009; Doody et al., 2017). However, the effectiveness of these strategies varies across landscape position, topography, and hydrological connectivity.

The Critical Source Area (CSA) concept suggests that a small fraction of the landscape (~20%) contributes the majority (~80%) of sediment yield (Pionke et al., 2000). CSAs are typically characterized by steep slopes, direct stream connectivity, and rapid runoff responses, making them dominant sediment sources (Tomer and Schilling, 2009; Doody et al., 2017). Overland flow is often a dominant mechanism for transporting eroded soil from CSAs into stream networks, where sediment load dynamics can be further shaped by hydrological processes such as dilution, deposition, tile drainage, and subsurface contributions (Pastén-Zapata et al., 2014; King et al., 2015). However, the role of these hydrological modifications in shaping in-stream sediment transport remains insufficiently understood, particularly in agricultural settings where both surface and subsurface pathways interact to redistribute sediment. Understanding these linkages is essential for accurately predicting in-stream sediment concentrations and assessing the effectiveness of erosion mitigation strategies. However, effective implementation of conservation strategies relies on correctly identifying CSAs first - without precise spatial targeting, erosion control efforts may be ineffective or misallocated (Giri et al., 2016). Thus, developing robust, data-driven approaches to pinpoint high-risk sediment sources is essential for implementing erosion mitigation strategies.

Soil conservation practices—such as conservation tillage, cover crops, and contour farming—can effectively reduce sediment transport in areas where overland flow velocities are low, allowing deposition before reaching streams (Gumiere et al., 2011; Fryirs, 2013). However, in steep terrain ($\geq 10\%$ slopes), high flow velocities and short retention times reduce their effectiveness, allowing continued sediment transport despite mitigation efforts (Boardman and Poesen, 2006). Fields with direct hydrological connections to streams contribute significantly more sediment than isolated fields, where material can settle before entering waterways (Li et al., 2021; U.S. Environmental Protection Agency, 2015).

While conservation practices at the plot or field scale have been widely studied (Maetens et al., 2012; Her et al., 2015), CSA identification remains rarely validated through long-term, high-



82 resolution sediment monitoring. As a result, the true effectiveness of erosion mitigation
83 strategies remains poorly constrained at the catchment scale, and the influence of overland
84 flow and sediment redistribution on conservation outcomes is still unclear (Doody et al., 2017,
85 Van Oost et al., 2007; Verstraeten et al., 2002). This gap in understanding how sediment is
86 transported from fields to stream networks limits the ability to assess conservation
87 effectiveness at early transport stages. Long-term studies assessing the interaction between
88 surface and subsurface transport in sediment connectivity remain scarce, despite advances in
89 erosion monitoring.

90 Peak flow, turbidity, and sediment load are influenced by hydrological processes and sediment
91 dynamics as overland flow transitions to in-stream conditions. At the in-stream scale,
92 subsurface flow contributions dilute sediment-water suspension, reducing turbidity and
93 sediment concentrations, particularly in catchments with groundwater discharge or wetland
94 buffering (Pastén-Zapata et al., 2014; King et al., 2015; Exner-Krittidge et al., 2016). However,
95 peak flow often increases due to wetland, spring, and subsurface flow contributions,
96 amplifying baseflow into stream networks (Blann et al., 2009).

97 Tile drainage systems further complicate sediment transport dynamics by bypassing
98 traditional sediment retention mechanisms, allowing fine sediments to enter streams directly
99 (Gentry et al., 2007; Rittenburg et al., 2015). Additionally, unmonitored diffuse overland flow
100 paths increase uncertainty in linking hillslope-scale erosion control to in-stream sediment
101 loads (Sharpley et al., 2009; Doody et al., 2017).

102 To address these knowledge gaps, this study leverages a decade-long, high-resolution dataset
103 from the Hydrological Open Air Laboratory (HOAL) in Austria (Blöschl et al., 2016), providing a
104 unique opportunity to assess conservation effectiveness at both field and catchment scales.
105 In particular, we examine how sediment transport processes operate across different spatial
106 scales, tracking changes from overland flow contributions at the hillslope scale to in-stream
107 sediment transport at the catchment scale. We examine how land management, topography,
108 and hydrological pathways influence sediment fluxes across multiple agricultural fields
109 differing in slope gradients, location within the catchment, and connectivity to the stream
110 network. A key focus is on identifying CSAs where non-erosive cultivation could significantly
111 reduce sediment export to the stream. Thus, we aim to address the following key research
112 questions:

- 113 • Which field characteristics determine the effectiveness of non-erosive cultivation
114 practices in reducing turbidity, sediment load, and overland flow?
- 115 • To what extent can a shift in cultivation practices mitigate sediment yield and water
116 fluxes?
- 117 • How do peak flow, turbidity, and sediment load change across spatial scales, from
118 overland flow inputs to in-stream monitoring stations, and what scale-dependent
119 hydrological and sediment transport processes drive these changes?



2. Study Area and Data

2.1 Study Area

The HOAL is a 66 ha agricultural catchment located in Petzenkirchen, Lower Austria (Figure 1). It is situated in a humid temperate climate, with a mean annual temperature of 9.5°C and mean annual precipitation of 823 mm (1990–2014), peaking during summer convective storms. These high-intensity precipitation events frequently trigger overland flow, which serves as a key driver of sediment mobilization and transport within the catchment (Blöschl et al., 2016).



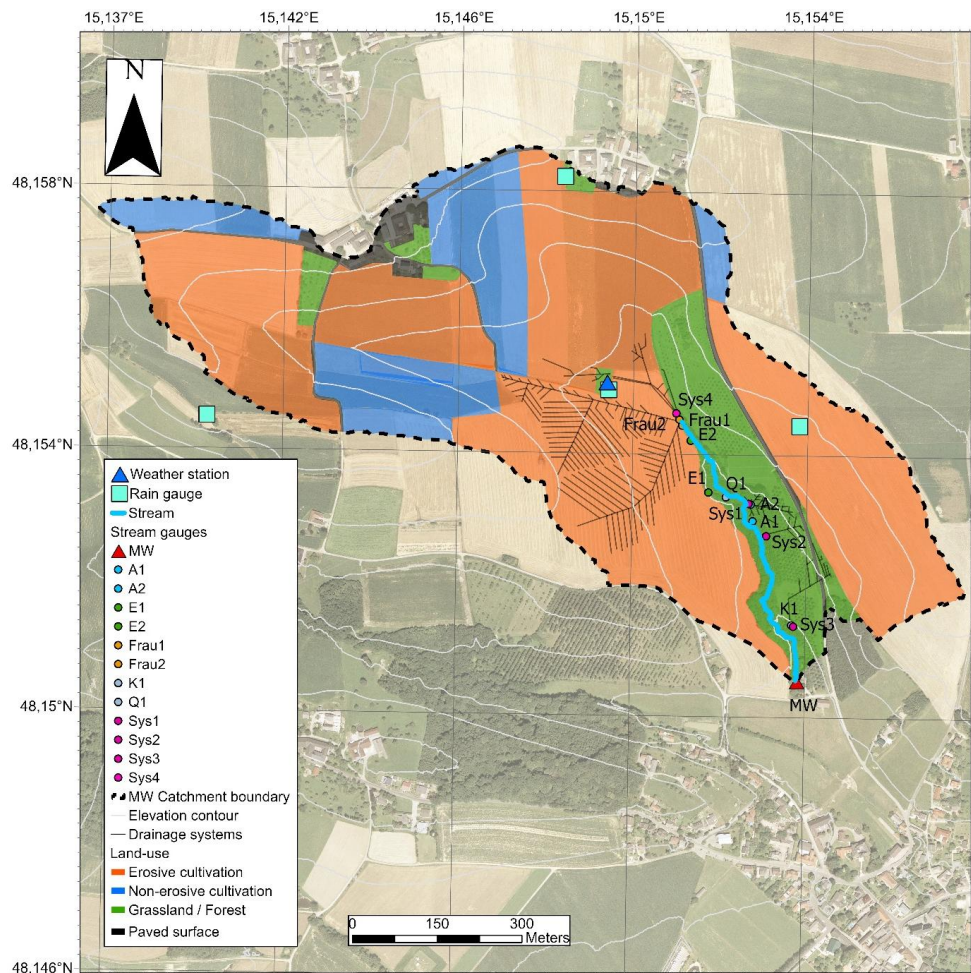
Figure 1: Aerial photograph of the 66 ha Hydrological Open Air Laboratory (HOAL) in lower Austria. Red line indicates the topographic catchment boundary, blue line indicates the main stream of the catchment. (Photo: BAW/Alexander Eder)

Elevation ranges from 268 to 323 m, with an average slope of 8%, creating spatial variability in overland flow generation and sediment connectivity. The underlying geology consists of Tertiary fine sediments of the Molasse zone, underlain by fractured siltstone, which influences subsurface drainage and sediment retention capacity. The dominant soil types—Cambisols (57%), Planosols (21%), Kolluvisols (16%), and Gleysols (6%)—exhibit moderate to poor infiltration capacities, with clay contents between 20–30%. Notably, Planosols and Gleysols contain low-permeability clay layers, leading to frequent waterlogging that enhances overland flow and erosion risk, particularly in intensively cultivated areas (Blöschl et al., 2016).

The Seitengraben, the main stream in the catchment, spans 620 m, with its outlet monitored at station MW. Water and sediment inputs originate from multiple surface and subsurface sources, which shape the sediment transport pathways.



142



143

144 *Figure 2: Overview map of the HOAL in Petzenkirchen, Austria. The map shows the spatial distribution of land-use classes*
145 *within the catchment for the year 2015 as an example. Additionally, it highlights the drainage systems, runoff measurement*
146 *stations, catchment boundary, the Seitengrabenbach stream, and the location of the rain gauges. (Credit: Credit: base map*
147 *layers from BAW-IKT; modifications and annotations by the authors)*

148 The main hydrological and sediment transport pathways include:

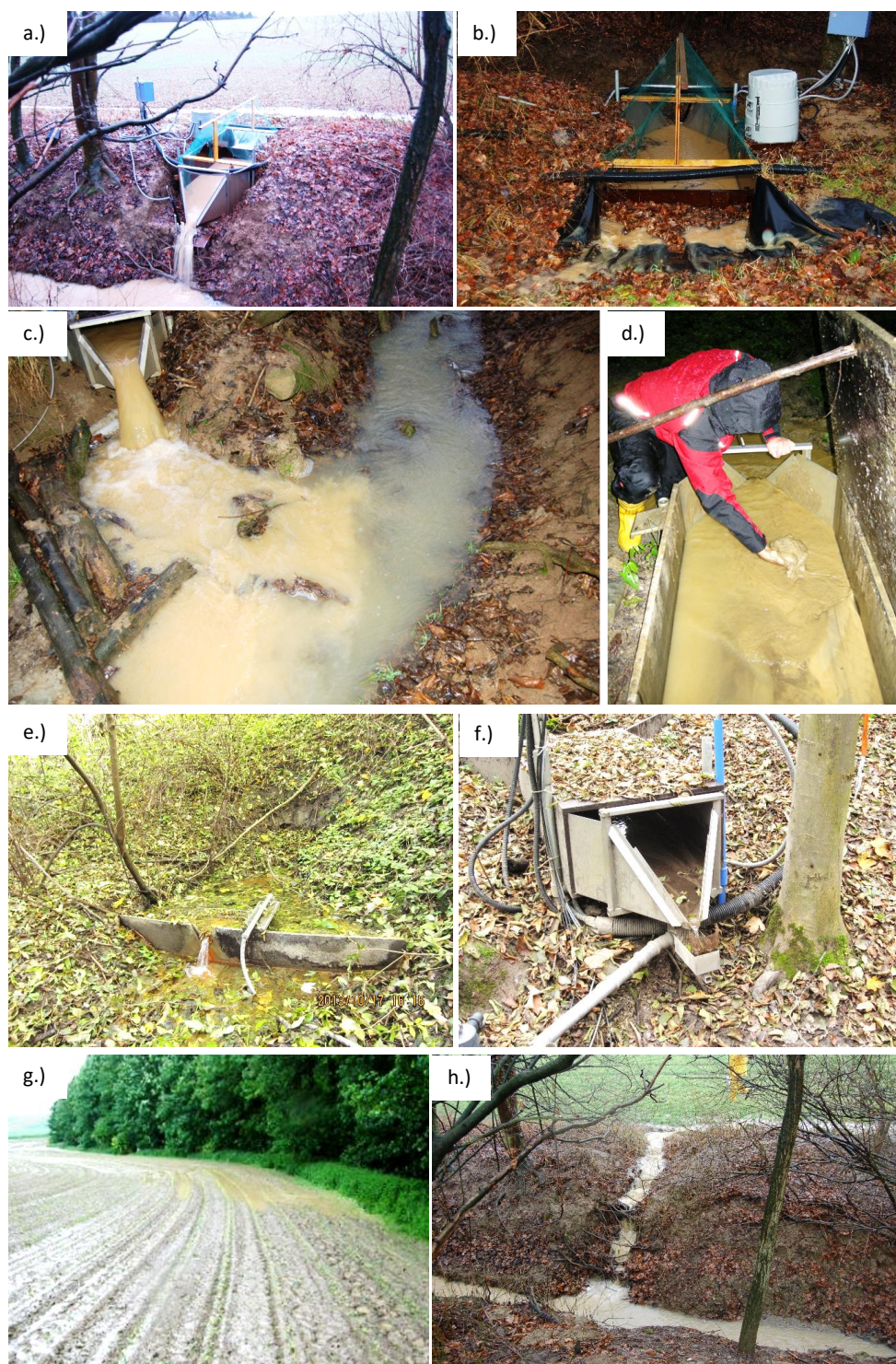
- 149
- Erosion Gullies (E1, E2) (Figure 3a and b): Overland flow is the dominant driver of
150 sediment transport during intense rainfall events, mobilizing eroded material from
151 agricultural fields and channelled through the erosion gullies, which serve as highly
152 connected sediment pathways to the stream.
 - Tile Drainage Systems (Sys1, Sys2, Sys3, Sys4, Frau1, Frau2) (Figure 3c and d): Installed
153 between the 1930s and 1950s to mitigate waterlogging, these systems bypass natural
154 sediment retention mechanisms, transporting fine-grained sediments directly to the
155 stream. Covering 15% of the catchment they facilitate the direct transport of eroded
156



157 material into the stream network (Blöschl et al., 2016). Among these, Frau 1 and Frau
158 2 are particularly relevant, as they demonstrably contribute to unmonitored sediment
159 fluxes. Unlike overland flow, which primarily mobilizes coarser sediment fractions, tile
160 drains transport fine sediment particles, which can accumulate within the drainage
161 pipes. During high-flow conditions, such as intense precipitation events, periods of
162 high antecedent soil moisture, or when preferential flow occurs through macropores,
163 these sediments can be flushed out, producing sudden pulses of sediment delivery to
164 the stream.

165 • Springs and Wetlands (Q1, K1, A1, A2) (Figure 3e and f): Perennial and intermittent
166 spring discharges (Q1, K1) contribute to baseflow, generally diluting turbidity, though
167 colloidal sediment transport may occur under certain conditions. A1 and A2 function
168 as wetlands that periodically dry out, influencing local water retention and sediment
169 deposition dynamics rather than providing constant baseflow contribution.

170 In addition to monitored inflow pathways, several unmonitored diffuse inflow pathways
171 contribute to sediment transport in the catchment. During large runoff events, excess water
172 and sediment can enter the stream through unmonitored paths between monitored stations
173 E1 and E2 (Figure 3g), diffuse overland flow pathways that are not fully captured by monitoring
174 infrastructure, and subsurface tile drainage systems at Frau 1 and Frau 2 (Figure 3h). These
175 pathways may lead to undetected sediment fluxes to the stream.





177 *Figure 3: Sediment transport pathways in the Hydrological Open Air Laboratory (HOAL). a) Frontal view and b) rear view show*
178 *the erosion gully E2 that capture overland flow which is the dominant driver of sediment transport during intense rainfall*
179 *events. c) and d) show the tile drainage Frau 2 that transport fine sediment particles, which can accumulate within the*
180 *drainage pipes and can be flushed out during intense precipitation events, producing sudden pulses of unmonitored sediment*
181 *delivery to the stream. e) shows the perennial and intermittent spring discharge K1 that contribute to baseflow, generally*
182 *diluting turbidity. f) shows wetland flow at A1 that periodically dries out and influences local water retention and sediment*
183 *deposition rather than providing constant baseflow. g) shows diffuse overland flow pathways between monitored stations E1*
184 *and E2 that allow excess water and sediment to enter the stream during large runoff events, bypassing monitoring*
185 *infrastructure. h) shows unmonitored overland flow pathways delivering sediment directly to the stream, bypassing*
186 *monitoring systems. (Photos: BAW-IKT)*

187 The land-use within the catchment is predominantly agricultural (Figure 2), with 87% of the
188 area usually cultivated with winter wheat, maize, barley, and oilseed rape. The remaining land
189 comprises forest (6%), grassland (5%), and paved surfaces (2%).

190 Understanding how these sediment pathways interact under different land management
191 strategies is essential for identifying CSAs and evaluating their contributions to in-stream
192 sediment fluxes.

193 2.2 Instrumentation and data availability

194 Precipitation was available at one-minute temporal resolution using four OTT Pluvio² weighing
195 rain gauges, each with a 400 cm² collecting area. The gauges were strategically installed across
196 the catchment to capture spatial precipitation variability (Figure 2).

197 Runoff was monitored at the overland flow station E2, the catchment outlet MW, and
198 additional tributary stations using calibrated H-flumes equipped with Druck PTX1830 pressure
199 transducers, providing one-minute temporal resolution. These stations capture diverse runoff
200 generation and sediment transport pathways, including overland flow (E2), tile drainage
201 (Sys1–Sys4, Frau1, Frau2), wetlands (A1, A2), and springs (K1, Q1).

202 To complement discharge monitoring, turbidity measurements were conducted at MW, E1,
203 and E2 using WTW ViSolid optical sensors (Xylem Analytics Germany, 2018). These sensors
204 determine suspended sediment concentrations (mg/l) via scattered light and backscattering
205 techniques. To maintain accuracy, the sensors were equipped with an ultrasonic cleaning
206 system to prevent biofouling and contamination by sediment. The raw turbidity data was
207 calibrated using laboratory analyses of total suspended solids (TSS) from collected water
208 samples.

209 A comprehensive water sampling program was conducted from 2012 to 2022 to analyze
210 sediment dynamics. Manual samples were collected monthly at all discharge stations when
211 flow was present. For event-based sampling, ISCO 6712 automatic samplers (Teledyne ISCO,
212 2019) were deployed using station-specific thresholds (Blöschl et al., 2016; Szeles et al., 2024).
213 When water levels in the H-flumes exceeded pre-defined thresholds—adjusted based on
214 baseflow conditions—sequential one-liter samples were collected at intervals ranging from 15
215 minutes to 2 hours, depending on event duration. Sampling continued until all 24 bottles were
216 filled or water levels dropped below the threshold. Following each event, the samples were
217 refrigerated and replaced within three days to ensure data integrity. A comprehensive
218 description of the instrumentation and data availability is provided by Blöschl et al. (2016).



In addition to hydrological monitoring, detailed land management information was provided by farmers from 2012 to 2022. This dataset included crop rotation, fertilization regimes, along with records of tillage, sowing, and harvesting schedules for all parcels within the catchment.

3. Methods

3.1 Data preparation

Given the rapid runoff response of the catchment to precipitation (Chen et al., 2020), discharge data at MW and E2 was analysed at a 5-minute resolution to improve temporal accuracy. Rainfall measurements from the four OTT Pluvio² gauges were averaged, as variations between them were minor. The original one-minute precipitation data was aggregated into 5-minute intervals by summing the recorded values.

To quantify the rainfall erosive potential, the erosivity index El_{30} was calculated. El_{30} represents the product of the total kinetic energy of a rainfall event and its maximum 30-minute rainfall intensity (Wischmeier and Smith, 1978). The calculation follows the equation (1):

$$El_{30} = \sum_{i=1}^m E_i \cdot I_{30,i} \quad (1)$$

where El_{30} is the rainfall erosivity factor ($\text{MJ mm ha}^{-1} \text{ h}^{-1}$), E_i is the total kinetic energy per rainfall event (MJ m^{-2}), I_{30} is the maximum 30-minute rainfall intensity within the event (mm h^{-1}), and m represents the number of rainfall events.

Sediment load was estimated by multiplying flow data from MW and E2 with turbidity measurements.

In terms of agricultural data, the main crops present in the study catchment between 2012 and 2022 included bare soil, soybean, potato, winter wheat, winter barley, maize, and cover crops such as clover grass and Lucerne. Following the classification outlined in the Austrian Agricultural Environmental Programme (ÖPUL) and Soil Erosion Evaluation Report (BML, 2021), these crops were categorized into erosive and non-erosive types. Erosive crops included bare soil, soybean, potato, and maize, while non-erosive crops comprised winter wheat, winter barley, and cover crops. Crop statistics of arable land for the study period are summarized in Table 1.

Table 1: Crop statistics of arable land between 2012 and 2022. The classification into erosive and non-erosive crop types was done according to the Austrian Agricultural Environmental Programme (ÖPUL) and Soil Erosion Evaluation Report (BML, 2021).

Year	Erosive Cultivation		Non-erosive Cultivation	
	Area (ha)	Area (%)	Area (ha)	Area (%)
2012	1.7–53.3	3.0–92.8	4.2–55.7	7.23–97.0
2014	13.4–52.1	23.4–90.8	5.3–44.0	9.2–76.6
2015	13.4–55.9	23.4–90.8	1.5–44.0	2.6–76.6
2016	1.1–56.1	1.9–97.7	1.3–56.3	2.3–98.1
2017	1.1–55.2	1.9–96.1	2.2–56.3	3.9–98.1
2018	10.6–55.3	18.4–96.3	2.1–46.9	3.7–81.6
2019	7.7–56.5	13.4–98.4	0.9–49.7	1.6–86.6
2020	7.7–52.6	13.4–91.7	4.8–49.7	8.3–86.6



2021	6.3–51.5	11.0–89.7	5.9–51.0	10.3–89.0
2022	3.4–43.6	5.9–76.0	13.8–54.0	24.0–94.1

250

251 3.2 Event separation

252 At the E2 station, hydrological events were measured exclusively during periods of overland
253 flow generation triggered by precipitation events, aligning with findings from previous studies.

254 To identify periods of direct flow at the MW station in the time series, we applied an
255 automated recursive digital filter (Nathan and McMahon, 1990; Arnold et al., 1995). This
256 approach is particularly well-suited for our study catchment, given its demonstrated
257 effectiveness in separating quick response flows from baseflows (Eder et al., 2010). Prior to
258 applying the digital filter, noisy discharge data were smoothed using a moving average filter
259 with a 5-minute window size.

260 The recursive digital filter is governed by the following equation (2):

$$261 \quad q_t = \beta \cdot q_{t-1} + \frac{(1+\beta)}{2} \cdot (Q_t - Q_{t-1}) \quad (2)$$

262 where q_t is the filtered quick response (event water) at time step t , Q_t is the total streamflow,
263 and β is the filter parameter. Following the recommendations of Nathan and McMahon (1990)
264 and Arnold et al. (1995), the value of β was set to 0.95, which was verified as appropriate for
265 the catchment through visual data inspection.

266 In defining hydrological events for our study, we followed a similar approach to Eder et al.
267 (2010). An event was considered to begin when streamflow increased above baseflow and
268 ended when only baseflow contributed to discharge, even if baseflow sediment
269 concentrations remained elevated. To ensure that small fluctuations did not lead to an
270 excessive number of minor events, additional thresholds were applied: the maximum
271 discharge of an event had to reach at least 5 ls^{-1} , the increase in discharge from its preceding
272 value had to exceed 2 ls^{-1} , and the peak turbidity during the event had to surpass 100 mg l^{-1} .
273 These criteria effectively minimized the inclusion of low-flow events with negligible suspended
274 sediment transport.

275 3.3 Event selection

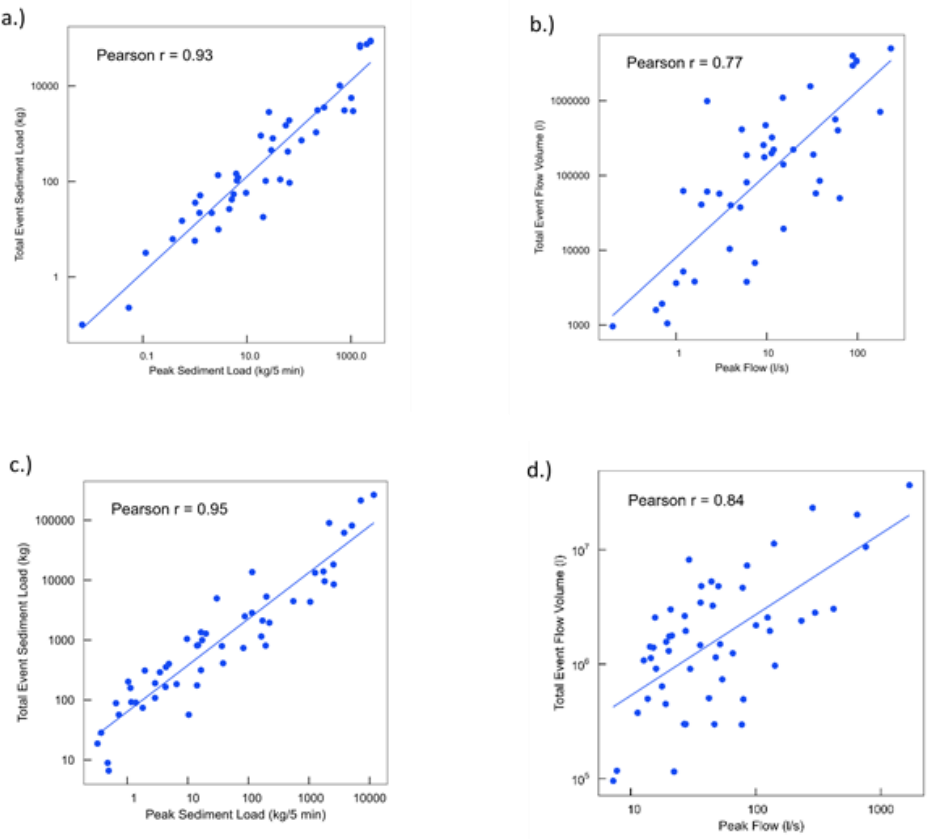
276 Between 2012 and 2022, we identified 255 events at MW and 85 at E2. However, while MW
277 events were consistently recorded, frequent sensor failures at E2 (e.g., turbidity sensors, flow
278 sensors, ISCO samplers) reduced the number of fully recorded events to 22. Most missing data
279 affected the rising or falling limb of hydrographs and turbidigraphs, limiting the dataset for E2.

280 To address scale effects between overland flow at E2 and in-stream dynamics at MW, we
281 matched corresponding E2 events with MW events whenever possible. Given the strong
282 correlations observed between peak values and total event values at both stations (Figure 4),
283 peak values were used as proxies to expand the dataset from 22 to 55 events at E2. This
284 approach facilitated a more comprehensive cross-scale comparison while mitigating the
285 impact of missing data at E2.



286 Statistical validation confirmed the reliability of peak values as event proxies. At E2, peak flow
287 and total event flow were strongly correlated ($r = 0.77$, Figure 4a), while peak sediment load
288 (kg/5 min) and total event sediment load (kg) exhibited an even stronger correlation ($r = 0.93$,
289 Figure 4b). At MW, these relationships were even more pronounced ($r = 0.84$ and $r = 0.95$,
290 Figures 4c and 4d, respectively). These findings align with previous research (e.g., Skålevåg et
291 al., 2024), demonstrating that peak flow and peak sediment load reliably characterize event-
292 scale sediment transport in highly responsive catchments.

293 We excluded 2013 from the analysis, as stream maintenance and excavator work at MW's
294 right bank artificially increased sediment loads, biasing the dataset. While E2 measurements
295 remained unaffected, the lack of reliable MW data precluded its use for that year.



296
297 *Figure 4: Relationship between (a) peak sediment load (kg/5 min) and total event sediment load (kg) at site E2, (b) peak flow*
298 *(l/s) and total event flow volume (l) at site E2, (c) peak sediment load (kg/5 min) and total event sediment load (kg) at site*
299 *MW, (d) peak flow (l/s) vs. total event flow volume (l) at site MW, with data points corresponding to individual events. Both*
300 *axes are displayed on a logarithmic scale, and the blue line indicates the linear regression fit. The Pearson correlation*
301 *coefficient (r) is displayed in each panel.*

302 **3.4 Catchment Segmentation**

303 In the HOAL, sediment transport is highly event-driven and influenced by a complex
304 interaction of hydrological connectivity, land management, and topography. Observations



305 from field visits, photographic evidence, and previous hydrological modelling studies (Strauss
306 et al., 2007) confirm that sediment transport rates are not only influenced by local field
307 conditions (e.g., topography, cultivation) but also by the spatial arrangement of fields within
308 the catchment.

309 Two primary overland flow pathways transport sediment from agricultural fields to the
310 stream, merging in the flat convergence zone in area C before reaching the E2 station (Figure
311 5). The steep slope of flowpath 2 promotes higher flow velocities and greater sediment
312 transport capacity than flowpath 1. Prior to reaching overland flow station E2, flowpath 2
313 traverses area GW9— a steeply inclined area that may act either as a sediment source or a
314 sink, depending on its vegetative cover, which alternates between erosive and non-erosive
315 cultivation. Similarly, flowpath 1 intersects area C, a comparatively flatter area where
316 sediment may be deposited or mobilized further, depending primarily on cultivation practices.

317 This segmentation of the HOAL catchment is based on the presence of these two distinct
318 flowpaths, each contributing overland flow and sediment to the same outlet (E2) but following
319 different trajectories through the catchment. Crucially, the final area traversed by flowpath 1
320 is flat and long, while that of flowpath 2 is steep and shorter. This configuration provides an
321 ideal natural experiment to assess how cultivation type (erosive vs. non-erosive) interacts with
322 terrain steepness to influence sediment and water retention in the agricultural landscape. It
323 allows for the isolation of topographic and cultivation type effects on sediment yield along key
324 hydrological flowpaths.

325 To systematically evaluate the spatial influence of different areas with distinct characteristics
326 on sediment yield at E2, we segmented the HOAL catchment into four distinct zones (Figure 5
327 and Table 2). This classification allows us to quantify how slope, distance, and connectivity
328 influence sediment yield, facilitating a spatially explicit assessment of erosion hotspots.

- 329
- 330 • Area A: This zone represents the source of flowpath 1, consisting of agricultural fields
331 within a larger sub-catchment with moderate slopes (weighted mean: 9.7%) and a
greater distance from the stream (weighted mean: 1112 m).
 - 332 • Area B: The source of flowpath 2, characterized by agricultural fields with steeper
333 slopes (weighted mean: 10.3%), and a medium distance from the stream (weighted
334 mean: 840 m).
 - 335 • Area GW9: This area represents the final agricultural field before flowpath 2 merges
336 with flowpath 1 in Area C. It is situated at a moderate distance from the stream
337 (weighted mean: 763 m) and has a very steep slope (weighted mean: 11.5%).
 - 338 • Area C: The final transition zone where both flowpath 1 and flowpath 2 converge
339 before entering the stream. This area is flat (weighted mean: 7.2%) and in immediate
340 proximity to the stream (weighted mean: 492 m).

341 By integrating this framework with high-resolution sediment monitoring, we can directly
342 identify high-risk areas and evaluate their contributions to both overland flow and in-stream
343 sediment transport. Furthermore, this enables a targeted evaluation of conservation
344 effectiveness along key flow pathways, particularly in high-connectivity areas. It also lays the
345 foundation for analyzing scale-dependent sediment transport, addressing our objective of
346 identifying CSAs while setting the stage for cross-scale sediment flux analysis.

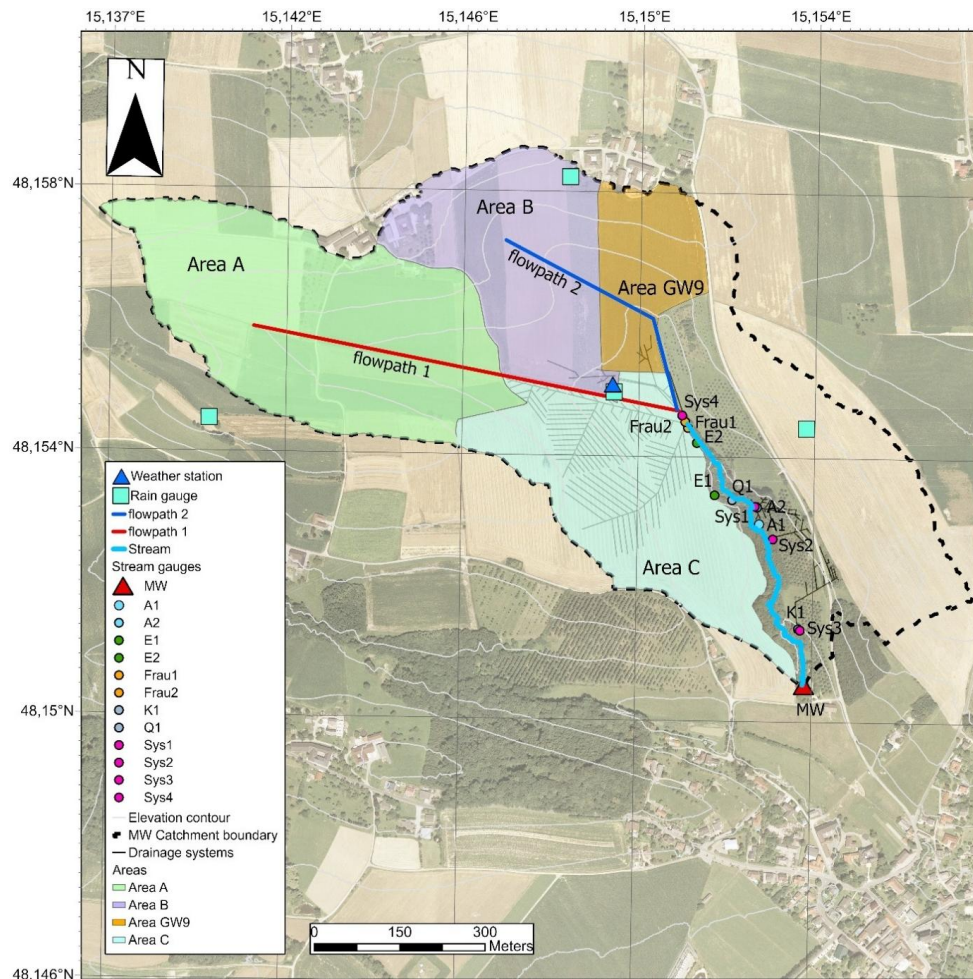


Figure 5: The map illustrates the division of the HOAL catchment into four distinct categories based on topographical and hydrological characteristics: (A) Green – medium steepness, located far from the Seitengrabenbach stream; (B) Violet – high steepness, situated medium distant to the stream; (GW9) Orange – high steepness, situated close to the stream; and (C) Violet – flat terrain near the stream. Additionally, the map highlights the two main overland flow paths. (Credit: Credit: base map layers from BAW-IKT; modifications and annotations by the authors)

Table 2: Mean weighted slope (%) and flow length (m) for the analyzed areas (A, B, GW9, and C). The slope represents the weighted mean terrain slope, while the flow length indicates the weighted mean distance water travels over the surface before reaching the overland flow measuring station E2.

	Area A	Area B	Area GW9	Area C
Slope (%)	9.7	10.3	11.5	7.2
Flow length (m)	1112	840	763	492

3.5 Statistical analysis

To evaluate the influence of cultivation type (erosive vs. non-erosive) on hydrological parameters, we applied the Kruskal-Wallis rank sum test (Kruskal and Wallis, 1952) to analyse differences in peak flow, peak turbidity, and peak sediment load across the study areas A, B,



361 GW9, and C at the overland flow measurement E2 station during 55 erosive events. The effect
362 size ϵ^2 (Tomczak and Tomczak, 2014) was computed to quantify the proportion of variance
363 explained by cultivation type, with p-values greater than 0.05 indicating statistically non-
364 significant effect.

365 To assess hydrological and land cultivation interdependencies, Spearman correlation
366 coefficients were calculated separately for overland flow (hillslope-scale) and in-stream
367 measurements (catchment-scale). For each event, peak values of hydrological and sediment-
368 related variables—such as El_{30} , peak flow, turbidity, and sediment load—were then correlated
369 with the percentage of area cultivated with erosive crop species within each classified area.
370 This approach aimed to identify how rainfall intensity and land cultivation practices affect
371 hydrological responses and sediment transport at different spatial scales. The overland flow
372 correlation matrix captured direct overland flow effects, while the in-stream correlation
373 matrix integrated multiple hydrological contributions. This comparison enabled an evaluation
374 of how land management and hydrological processes influence sediment transport across
375 spatial scales within the study catchment.

376 4. Results

377 4.1 Cultivation Type Effects on Hydrological Response

378 4.1.1 Upstream erosion gully

379 At the E2 station, peak flow, peak turbidity, and peak sediment load exhibited both similarities
380 and spatial variability across study areas A, B, GW9, and C, reflecting distinct hydrological
381 conditions and sediment connectivity pathways.

382 In areas A, B, and GW9, peak turbidity (Figure 6a-c and Table 3) and peak sediment load (kg/5
383 min) (Figure 6e-g and Table 3) showed no significant differences ($p > 0.05$) between erosive
384 and non-erosive cultivation types. For peak sediment load, the median sediment load values
385 in fields with non-erosive cultivation were generally higher than those in fields with erosive
386 cultivation. However, the Kruskal-Wallis test confirmed that these differences were not
387 statistically significant, with small effect sizes in all three areas. Similarly, peak turbidity values
388 showed no consistent trend between cultivation types, with some areas exhibiting higher
389 values under non-erosive cultivation and others under erosive practices. These results suggest
390 that non-erosive cultivation was less effective in reducing peak turbidity and peak sediment
391 load (kg/5 min) in agricultural areas characterized by steeper slopes and greater distances
392 from the stream — specifically in Area A (moderate slope ~9.7%, distant ~1110 m), Area B
393 (steeper slope ~10.3%, medium distance ~840 m), and Area GW9 (very steep slope ~11.5%,
394 medium distance ~760 m).

395 In contrast, Area C, characterized by a relatively flat slope (7.2%) and close proximity to the
396 stream (<500 m), exhibited a pronounced sensitivity of the hydrological response to
397 cultivation type, with non-erosive practices significantly reducing peak turbidity (Figure 6d)
398 and sediment load (Figure 6h). Statistical analysis confirmed these reductions as highly
399 significant, yielding large effect sizes for both parameters (Table 3).

400 Under erosive cultivation, median peak sediment load was 29.5 kg/5 min, approximately ~9.5
401 times higher than under non-erosive conditions (2.8 kg/5 min), with a statistically significant



402 effect ($p = 0.0022$) and a large effect size ($\epsilon^2 = 0.1545$), indicating that cultivation type
403 accounted for ~15.5% of the variation in sediment load. Similarly, peak turbidity reached 22.7
404 g/L under erosive conditions, about ~3.8 times higher than under non-erosive practices (4.7
405 g/L), with a highly significant effect ($p = 0.0001$) and a large effect size ($\epsilon^2 = 0.2616$), explaining
406 ~26.2% of the variation in peak turbidity.

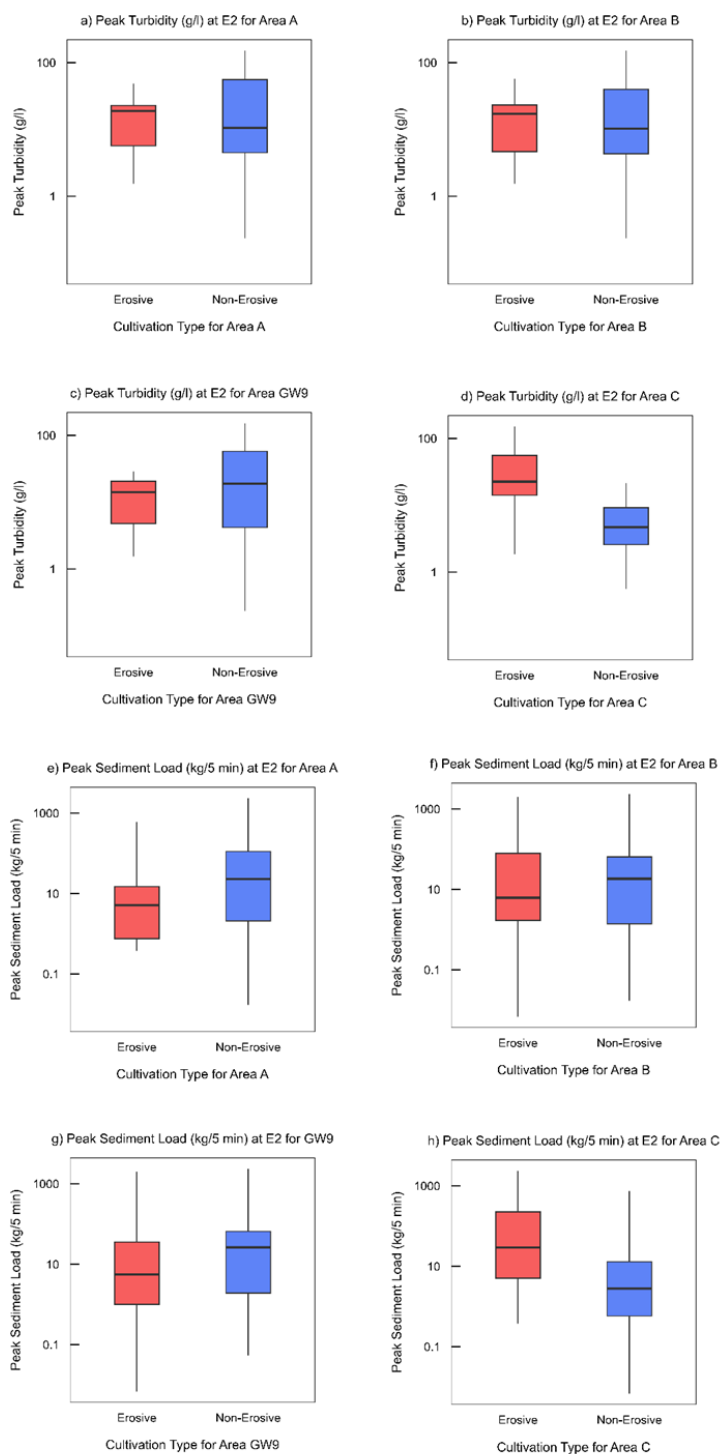




Figure 6: Boxplots showing the distribution of peak turbidity (g/l), peak sediment load (kg/5 min) at overland flow measurement site E2 for different cultivation types (erosive vs. non-erosive) in areas A, B, GW9, and C. The median and interquartile range are displayed for each category. The y-axis is on a logarithmic scale. Panels correspond to: (a) Peak Turbidity at E2 for Area A, (b) Peak Turbidity at E2 for Area B, (c) Peak Turbidity at E2 for Area GW9, (d) Peak Turbidity at E2 for Area C, (e) Peak Sediment Load at E2 for Area A, (f) Peak Sediment Load at E2 for Area B, (g) Peak Sediment Load at E2 for Area GW9, (h) Peak Sediment Load at E2 for Area C.

In all areas, peak flow (Figure A1 and Table 3) did not differ significantly ($p > 0.05$) between erosive and non-erosive cultivation types. While median values varied across locations, the Kruskal-Wallis test confirmed that these differences were not statistically significant, with small effect sizes (ϵ^2) in all areas. These results indicate that cultivation type does not play a major role in peak flow generation across all agricultural areas with unique hydrological characteristics, regardless of differences in slope, flow length, or proximity to the stream.

Table 3: Comparison of peak sediment load (kg/5 min), peak turbidity (g/l), and peak flow (l/s) between erosive and non-erosive cultivation types across different areas at the overland flow measuring station E2. Bold print indicates statistical significance (* $P < 0.05$; ** $P < 0.01$; *** $P < 0.001$) and a large magnitude of the effect size (ϵ^2).

Hydrological Parameter	Area	Cultivation Type	Peak Value	Kruskal-Wallis χ^2 (df = 1)	p-value	Effect Size (ϵ^2)	Magnitude
Sediment Load (kg/5 min)	A	Erosive	19.7	0.0823	0.7743	-0.017	Small
		Non-Erosive	11.5				
	B	Erosive	16.7	0.3164	0.5738	-0.0127	Small
		Non-Erosive	14.2				
	GW9	Erosive	14.2	1.7427	0.1868	0.0138	Small
		Non-Erosive	19.0				
	C	Erosive	22.7	15.126	0.0001	0.2616	Large
		Non-Erosive	4.7				
Turbidity (g/l)	A	Erosive	19.7	0.0823	0.7743	-0.017	Small
		Non-Erosive	11.5				
	B	Erosive	16.7	0.3164	0.5738	-0.0127	Small
		Non-Erosive	14.2				
	GW9	Erosive	14.2	1.7427	0.1868	0.0138	Small
		Non-Erosive	19.0				
	C	Erosive	22.7	15.126	0.0001	0.2616	Large
		Non-Erosive	4.67				
Flow (l/s)	A	Erosive	2.2	3.9946	0.0457	0.0555	Small
		Non-Erosive	9.2				
	B	Erosive	4.0	0.7341	0.3916	-0.0049	Small
		Non-Erosive	6.0				
	GW9	Erosive	5.8	0.3019	0.5827	-0.0129	Small
		Non-Erosive	6.0				
	C	Erosive	6.0	1.1366	0.2864	0.0025	Small
		Non-Erosive	5.9				

423

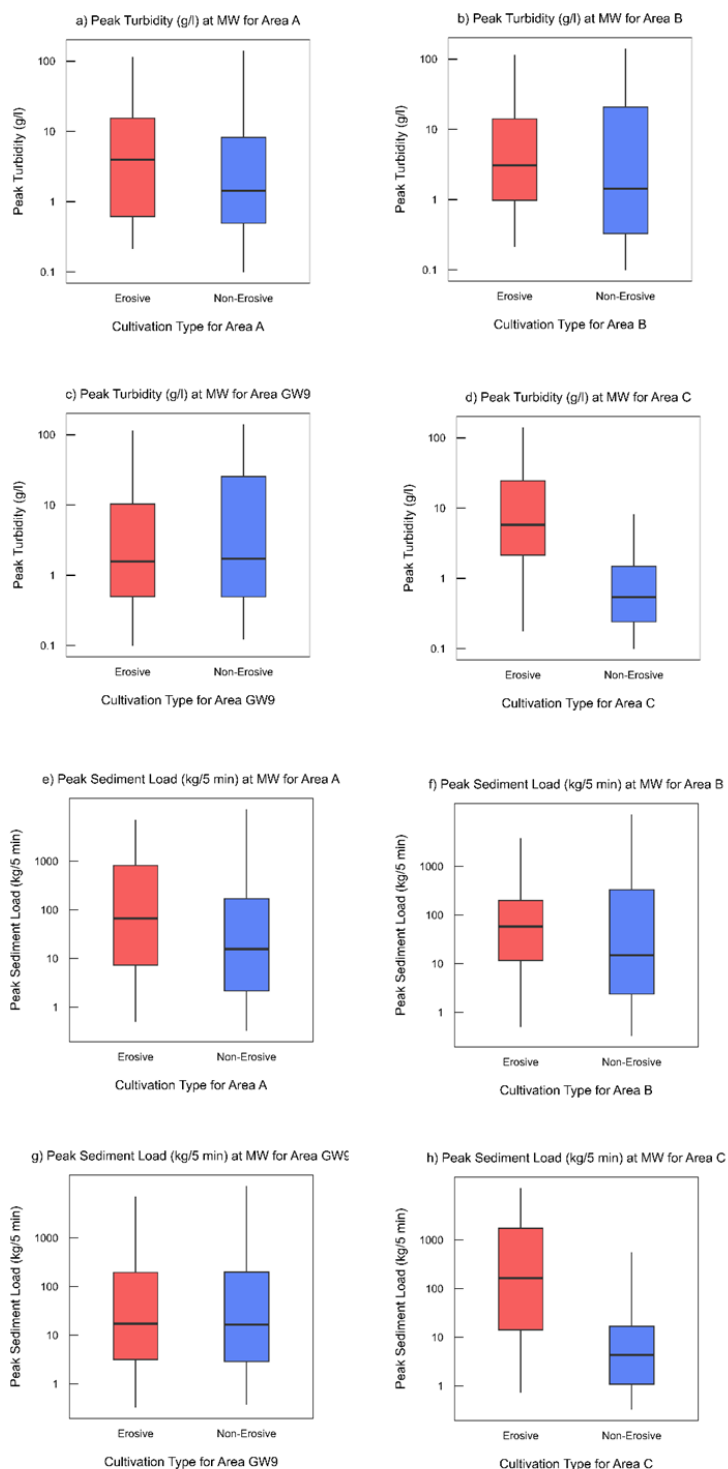
4.1.2 Catchment outlet

The MW station exhibited sediment dynamics similar to those observed at the E2 station, with no significant differences in peak turbidity (Figure 7a-c), peak sediment load (Figure 7e-g), or



427 peak flow (Figure A2a-c) for areas A, B, and GW9. While non-erosive cultivation generally
428 resulted in lower median values for peak turbidity and sediment load, the absence of a
429 consistent trend suggests that land management practices in steeper (~10–12% slope),
430 medium-distance (~750–850 m) and moderately steep (~9.6% slope), distant (>1000 m)
431 agricultural areas have limited influence on sediment transport and turbidity at the catchment
432 outlet.

433 In contrast, Area C displayed a significant response to cultivation practices, with erosive
434 cultivations leading to pronounced increases in both peak turbidity (Figure 7d) and peak
435 sediment load (Figure 7h), mirroring the trends observed at the E2 station. Events associated
436 with erosive cultivation resulted in peak sediment loads that were 38 times higher than under
437 non-erosive conditions (163 kg/5 min vs. 4.3 kg/5 min), with a significant effect ($p = 0.0003$)
438 and a large effect size ($\epsilon^2 = 0.245$), indicating that cultivation type accounts for 24.5% of the
439 variability in sediment load at the MW station (Table 4). Similarly, peak turbidity was more
440 than 10 times higher under erosive conditions (5777 g/l) than under non-erosive cultivation
441 (537 g/l), with a large effect size ($\epsilon^2 = 0.2368$, $p = 0.0003$). These results indicate that in flat
442 agricultural areas (7.2% slope) near the stream (<500 m), non-erosive cultivation significantly
443 reduces both peak sediment load and peak turbidity at the catchment outlet.





445 *Figure 7: Boxplots showing the distribution of peak turbidity (g/l) and peak sediment load (kg/5 min) for different cultivation*
 446 *types (erosive vs. non-erosive) at in-stream measurement site MW across areas A, B, GW9, and C. The median and interquartile*
 447 *range are displayed for each category. The y-axis is on a logarithmic scale. Panels correspond to: (a) Peak Turbidity at E2 for*
 448 *Area A, (b) Peak Turbidity at E2 for Area B, (c) Peak Turbidity at E2 for Area GW9, (d) Peak Turbidity at E2 for Area C, (e) Peak*
 449 *Sediment Load at E2 for Area A, (f) Peak Sediment Load at E2 for Area B, (g) Peak Sediment Load at E2 for Area GW9, (h) Peak*
 450 *Sediment Load at E2 for Area C.*

451 Unlike at E2, where peak flow remained unaffected by cultivation type, the MW station
 452 exhibited a statistically significant increase in peak flow under erosive cultivation in Area C
 453 (Figure A2d). Median peak flow was approximately three times higher under erosive
 454 conditions (65.6 l/s) than under non-erosive practices (22.2 l/s), with a large effect size ($\epsilon^2 =$
 455 0.1571, $p = 0.0029$) (Table 4).

456 *Table 4: Comparison of peak sediment load (kg/5 min), peak turbidity (g/l), and peak flow (l/s) between erosive and non-*
 457 *erosive cultivation types across different areas at the in-stream measuring station MW. Bold print indicates statistical*
 458 *significance (* $P < 0.05$; ** $P < 0.01$; *** $P < 0.001$) and a large magnitude of the effect size (ϵ^2).*

Hydrological Parameter	Area	Cultivation Type	Peak Value	Kruskal- Wallis χ^2 (df = 1)	p-value	Effect Size (ϵ^2)	Magnitude
Sediment Load (kg/5 min)	A	Erosive	38.2	0.7026	0.4019	-0.0059	Small
		Non-Erosive	16.5				
	B	Erosive	87.3	1.7442	0.1866	0.0149	Small
		Non-Erosive	14.2				
	GW9	Erosive	17.2	0.0041	0.9489	-0.0199	Small
		Non-Erosive	16.5				
	C	Erosive	163.2	13.241	0.0003	0.245	Large
		Non-Erosive	4.3				
Turbidity (g/l)	A	Erosive	3977.7	0.8821	0.3476	-0.0024	Small
		Non-Erosive	1420.5				
	B	Erosive	3086.3	0.4811	0.4879	-0.0104	Small
		Non-Erosive	1420.5				
	GW9	Erosive	1575.9	0.3764	0.5395	-0.0125	Small
		Non-Erosive	1721.3				
	C	Erosive	5777.1	12.842	0.0003	0.2368	Large
		Non-Erosive	537.0				
Flow (l/s)	A	Erosive	36.0	0.11107	0.7389	-0.0178	Small
		Non-Erosive	36.7				
	B	Erosive	65.6	2.3986	0.1214	0.028	Small
		Non-Erosive	29.3				
	GW9	Erosive	36.7	0.57769	0.4472	-0.0084	Small
		Non-Erosive	29.3				
	C	Erosive	65.6	8.8537	0.0029	0.1571	Large
		Non-Erosive	22.2				

459



4.2 Hydrological and Land Cover Interdependencies in Overland Flow and In-Stream Measurements

4.2.1 Overland Flow Characteristics

The Spearman correlation analysis (Section 3.4) for overland flow (Figure 8) highlights that rainfall erosivity (El_{30}) is moderately associated with sediment load and turbidity. The moderate positive correlation of El_{30} with peak sediment load ($\rho = 0.58$) and peak turbidity ($\rho = 0.59$) suggests that more intense rainfall events lead to increased sediment mobilization and higher turbidity levels. The correlation between El_{30} and peak flow was weaker ($\rho = 0.40$), indicating that while El_{30} plays a role in overland flow generation, other factors also contribute to shaping flow responses.

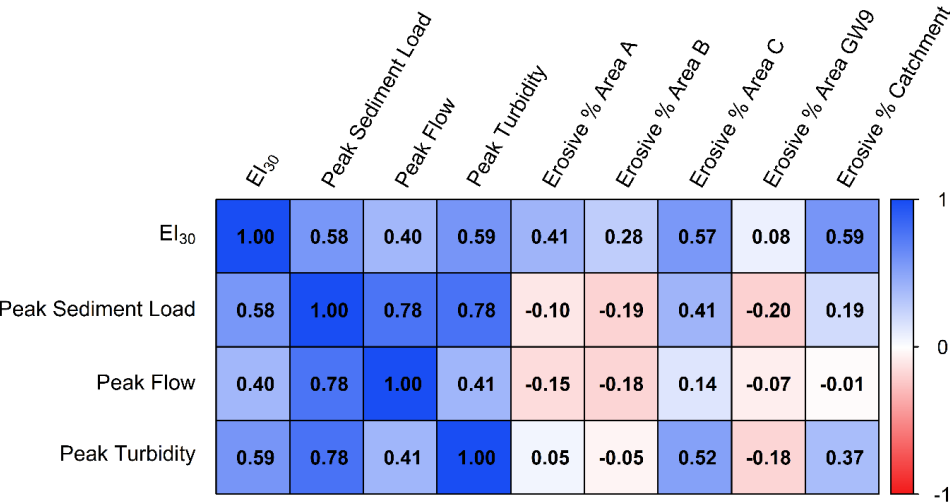


Figure 8: Spearman correlation matrix for overland flow measurements, showing the relationships between rainfall intensity (El_{30}), hydrological responses (peak sediment load (kg/5 min), peak turbidity (g/l), peak flow (l/s)), and erosive land cover in different catchment areas. Positive correlations are shown in blue, and negative correlations in red, with intensity representing the strength of the correlation.

Among the hydrological variables, a weak relationship was found between peak turbidity and peak flow ($\rho = 0.41$), suggesting that while flow magnitude influences turbidity, additional factors may contribute to turbidity variations as well.

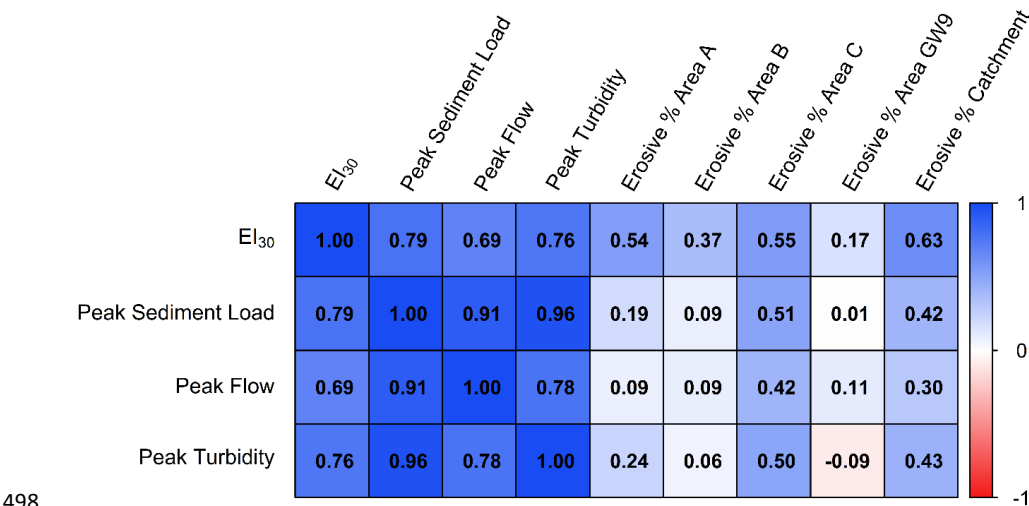
The influence of erosive land cover on hydrological responses varied across the catchment areas, with spatially heterogeneous relationships between land cover cultivations, and sediment transport dynamics. In Area A, erosive land cover exhibited no relationship with peak turbidity ($\rho = 0.05$). Area B and GW9 displayed even negative correlations between erosive land cover and both peak sediment load (Area B: $\rho = -0.19$, GW9: $\rho = -0.20$) and peak turbidity (Area B: $\rho = -0.05$, GW9: $\rho = -0.18$). These weak associations suggest that cultivation practices in these areas of the catchment may not have a significant impact on peak turbidity and peak sediment load, as their effect could be obscured by other factors. In contrast, Area C showed a positive correlation between erosive land cover and sediment load ($\rho = 0.41$) and turbidity ($\rho = 0.52$), indicating that in this particular area of the catchment, the type of land cover may exert a stronger influence on sediment transport dynamics.



489 The relationship between erosive land cover and peak flow was consistently weak and mostly
490 negative across all areas (Area A: $\rho = -0.15$, Area B: $\rho = -0.18$, Area C: $\rho = 0.14$, GW9: $\rho = -0.07$).
491 These results suggest that land cover alone does not strongly explain variations in peak flow.

492 **4.2.2 In-Stream Measurement Characteristics**

493 The correlation analysis for in-stream measurements (Figure 9) revealed a stronger influence
494 of rainfall intensity on hydrological responses compared to overland flow. El_{30} exhibited higher
495 correlations with peak sediment load ($\rho = 0.79$), peak turbidity ($\rho = 0.76$), and peak flow ($\rho =$
496 0.69), indicating that rainfall erosivity exerts a dominant control over hydrological and
497 sediment transport mechanisms within the catchment and stream network.



498
499 *Figure 9: Spearman correlation matrix for in-stream measurements, showing the relationships between rainfall intensity (El_{30}),*
500 *hydrological responses (peak sediment load (kg/5 min), peak turbidity (g/l), peak flow (l/s)), and erosive land cover in different*
501 *catchment areas. Positive correlations are shown in blue, and negative correlations in red, with intensity representing the*
502 *strength of the correlation.*

503 The relationships among hydrological parameters were also more pronounced in the in-
504 stream matrix than in overland flow (Figure 9). Peak flow and peak sediment load ($\rho = 0.91$)
505 and peak flow and peak turbidity ($\rho = 0.78$) exhibited strong associations, suggesting that
506 sediment and turbidity dynamics in the stream are primarily flow-driven.

507 The role of land cultivation in in-stream sediment dynamics varied across the catchment.
508 Correlations between erosive land cover and sediment transport variables were generally
509 consistent with overland flow, indicating that catchment sediment dynamics is primarily
510 governed by overland flow and land cover effects rather than diverse in-stream processes. In
511 Area A and B, erosive land cover exhibited a weak positive relationship with peak turbidity
512 (Area A: $\rho = 0.24$, Area B: $\rho = 0.05$) and peak sediment load (Area A: $\rho = 0.19$, Area B: $\rho = 0.09$).
513 In Area GW9, erosive land cover exhibited a weak negative correlation with peak turbidity ($\rho =$
514 -0.09) and showed no distinguishable relationship with peak sediment load. These weak
515 associations suggest that cultivation practices in areas A, B, and GW9 of the catchment do not
516 have a significant impact on overall peak turbidity and peak sediment load. In contrast, Area
517 C exhibited the highest correlations between erosive land cover and both peak sediment load



($p = 0.51$) and peak turbidity ($p = 0.50$) among all areas. While these correlations remain moderate, they may point to a relatively stronger association between land cover and sediment dynamics in this part of the catchment.

The correlation between erosive land cover and peak flow remained consistently weak or negative across all areas (Area A: $p = 0.09$, Area B: $p = 0.09$, Area C: $p = 0.42$, GW9: $p = 0.11$), further supporting the dominant role of rainfall erosivity ($p = 0.69$) in driving streamflow generation rather than direct land cover effects. These results align with findings from the overland flow analysis, reinforcing the idea that peak flow is primarily influenced by precipitation inputs and catchment-wide hydrological responses rather than catchment or localized land cover patterns.

5. Discussion

5.1 The Role of Cultivation Practices on Peak Flow, Turbidity and Sediment Load at the hillslope-scale

Our results indicate that the effectiveness of non-erosive cultivation practices in reducing peak turbidity and sediment load in overland flow is highly dependent on field location relative to the stream and topography. In steep (~10–12% slope) and medium-to-distant agricultural areas (750–1000+ m from the stream), non-erosive practices did not significantly reduce sediment transport (Figure 6 and Figure 7; Table 3 and 4).

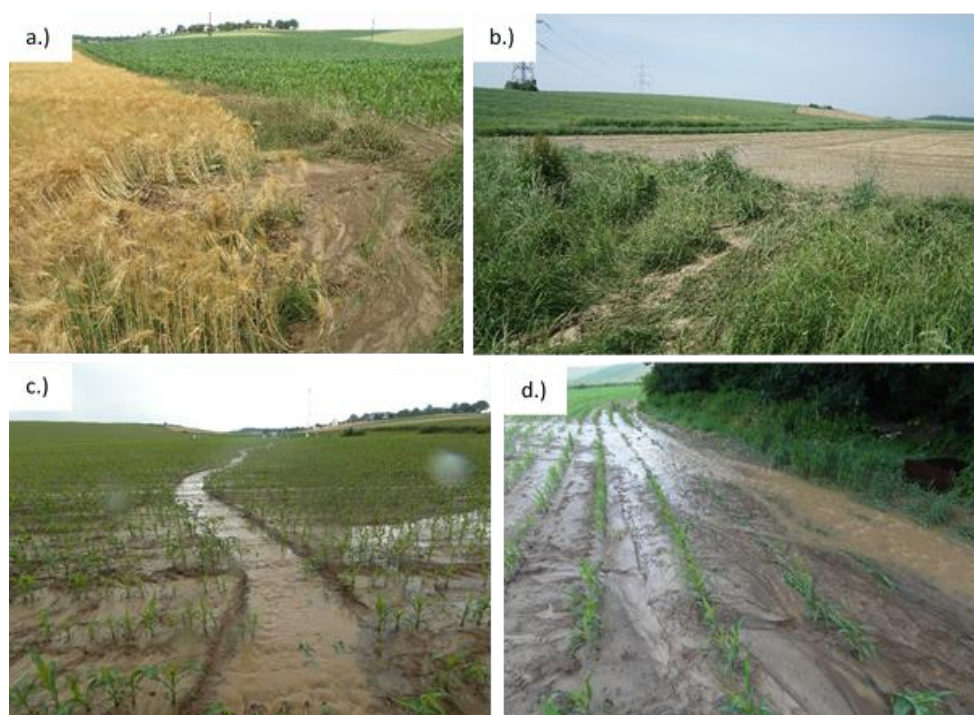
This aligns with previous studies (e.g., Boardman and Poesen, 2006), which emphasize that gravitational forces and high overland flow velocities in steep terrains enhance sediment detachment and transport. Even with increased vegetation cover, the steep topography and resulting high flow velocities in these areas likely promote continued sediment detachment, limiting the effectiveness of non-erosive cultivation in preventing soil erosion (Firoozi and Firoozi, 2024). Boardman and Poesen (2006) and Wu et al. (2018) demonstrated that sediment detachment intensifies in steep terrain due to accelerated overland flow, with runoff responses more dependent on infiltration capacity and surface roughness. This is supported by Zhang et al. (2020), who demonstrated that steeper slopes (>10%) experience enhanced soil loss, particularly when rainfall intensity is high. In flowpath 1, uninterrupted slopes (>10%) may accelerate overland flow, which may intensify sediment transport. As a result, non-erosive cultivation had minimal impact in these steep, medium-to-distant agricultural areas, as elevated flow velocities in these areas may sustain sediment detachment, thereby reducing the effectiveness of non-erosive cultivation in preventing soil erosion.

In contrast, non-erosive cultivation proved highly effective in flat agricultural areas close to the stream (7.2% slope, <500 m from the stream), significantly reducing turbidity (~3.8 times) and sediment load (~9.5 times). This aligns with findings from Lin et al. (2019), who demonstrated that winter wheat and cover crops can reduce sediment loss by up to 98.2% on moderate slopes, although their impact on total overland flow was limited. Similarly, Wu et al. (2019) found that wheat and other dense-cover crops effectively reduced sediment loss on moderate slopes (5–7%) but had limited ability to regulate total overland flow generation.

In Area C, vegetation effectively traps sediment before it reaches the E2 monitoring station. However, overland flow remains unchanged, as non-erosive practices primarily influence



559 sediment deposition rather than overland flow reduction. Here, vegetation density was
560 noticeably higher in non-erosive fields, as seen in field observations during event monitoring.
561 The denser root and canopy structure in non-erosive cultivation types like winter wheat
562 (Figure 10a) and cover crops (Figure 10b) compared to erosive cultivation types like maize
563 (Figure 10c and Figure 10d) slows sediment transport, allowing particles to settle because
564 overland flow slowed down due to the flatter terrain. Despite reducing turbidity and sediment
565 load, non-erosive practices had no impact on overland flow volume (Figure A1 and Table 3),
566 reinforcing that they regulate sediment transport rather than overland flow generation (Lin et
567 al., 2019).



568

569 *Figure 10: The images at the top (a, b) illustrate how overland flow and sediment erosion originate from erosive areas of the*
570 *catchment, such as a) maize fields or b) bare soil patches, where limited vegetation cover fails to intercept overland flow. As*
571 *the sediment-laden water moves downslope, it reaches a field with non-erosive cultivation (a) winter wheat or b) cover crops,*
572 *where the dense vegetation effectively leads to sediment deposition, preventing further transport toward the stream. The*
573 *images at the bottom (c, d) illustrate overland flow and sediment erosion between the weather station and the stream. The*
574 *affected Area C is cropped with early-stage maize, which is an erosive crop species and does not effectively hinder overland*
575 *flow, leading to increased overland flow and sediment transport. (Photos: BAW-IKT)*

576 The influence of non-erosive cultivation on overland flow generation remained negligible
577 across all monitored locations (Figure A1). This supports findings from Wu et al. (2018) and
578 Zhang et al. (2020), which demonstrated that rainfall characteristics and soil moisture, rather
579 than land management, was the dominant control on overland flow generation in agricultural
580 catchments. Our findings indicate that non-erosive cultivation alone is insufficient to regulate
581 overland flow, in steep as well as in flat terrains. Given the high sediment transport in flowpath
582 1, additional conservation measures—such as contour plowing, buffer strips to reduce
583 sediment connectivity—are necessary to complement non-erosive practices. These strategies



584 would more effectively reduce sediment transport and enhance infiltration, particularly in
585 steeper agricultural areas (Borin et al., 2005).

586 5.2 The Role of Cultivation Practices on Peak Flow, Turbidity, and Sediment Load at the 587 Catchment Outlet

588 Our results indicate that hydrological and sediment transport dynamics at the MW in-stream
589 monitoring site reflect contributions from multiple sources, including wetlands, springs,
590 subsurface flows, and direct overland flow from agricultural land. While the general
591 hydrological pattern observed at E2 persists, key differences emerge due to dilution and
592 additional flow contributions. Notably, in-stream sediment mobilization from riverbed and
593 riverbank erosion plays a negligible role in our catchment (Eder et al., 2014), suggesting that
594 the observed sediment loads are predominantly sourced from overland flow and subsurface
595 drainage pathways.

596 At the catchment outlet, peak flow increased between ~2.8 and ~11 times compared to E2,
597 indicating significant hydrological contributions from other flow contributions such as
598 wetlands, springs and tile drainages. This aligns with findings by Eder et al. (2014), who
599 demonstrated that subsurface flow and groundwater upwelling significantly contributed to
600 baseflow and peak discharge in the study catchment. The observed increase in peak flow
601 suggests that these additional flow contributions, which respond differently to precipitation
602 events, are critical in modulating stream discharge.

603 The magnitude of peak flow varied between erosive and non-erosive cultivation conditions at
604 Area C. While peak flow at E2 remained similar across both cultivation types, at MW, peak
605 flow was ~3 times higher under erosive compared to non-erosive conditions. Although non-
606 erosive cultivation may be generally associated with a ~20% reduction in overland flow (López-
607 Vicente and Navas, 2010), this trend was not observed at E2 in our study. Furthermore, the
608 observed increase in peak flow at MW cannot be fully explained by tile drainages, wetlands,
609 or springs, suggesting that unmonitored hydrological overland flow pathways play a larger role
610 than previously assumed.

611 Field observations during severe erosion events suggest that the E2 monitoring station
612 reached a capacity threshold, beyond which overland flow was no longer effectively captured.
613 Once this threshold was exceeded, a greater proportion of overland flow bypassed the
614 monitoring infrastructure through diffuse, unmonitored pathways, contributing directly to the
615 stream at MW. This interpretation aligns with hydrological connectivity and threshold
616 behavior studies (e.g., Saffarpur et al., 2016), which show that excess runoff can activate
617 alternative, less-monitored flow paths once critical flow thresholds are surpassed. As a result,
618 sediment and water inputs at MW during erosive events likely reflect both monitored
619 contributions from E2 and additional, unaccounted-for overland flow routed along these
620 alternative pathways.

621 At MW, peak turbidity decreased by ~5.4 to ~7.7 times relative to E2, indicating strong dilution
622 from wetlands, springs, and subsurface flow. This reduction exceeds typical values reported
623 for temperate agricultural watersheds (~3 to ~5 times, Sharpley et al., 2019), suggesting that
624 dilution processes in our catchment are particularly effective. Consistent with Vercruysse et



625 al. (2017), our findings confirm that groundwater, wetlands, and tributary inflows play a key
626 role in regulating downstream sediment concentrations.

627 Despite dilution, the relative impact of cultivation at Area C on peak turbidity persisted from
628 E2 to MW, emphasizing the dominant role of land management in controlling sediment
629 transport (Boardman and Poesen, 2006). Specifically, erosive cultivation in Area C resulted in
630 significantly higher peak turbidity at both E2 and MW, demonstrating that hillslope-scale
631 sediment detachment has a persistent downstream impact (Zhang et al., 2020). In contrast,
632 non-erosive cultivation in Area C effectively reduced peak turbidity at both monitoring sites,
633 supporting findings from Lin et al. (2019) and Wu et al. (2019) that conservation practices (e.g.,
634 cover crops) reduce sediment detachment but do not necessarily alter total overland flow
635 volumes.

636 While dilution lowered turbidity at MW, the relative difference between erosive and non-
637 erosive cultivation became more pronounced. Under erosive cultivation, median peak
638 turbidity at E2 was ~4 times higher than at MW, whereas under non-erosive conditions, it was
639 ~8.5 times higher at E2 compared to MW. Furthermore, at E2, median peak turbidity was ~4.5
640 times higher for erosive compared to non-erosive conditions, while at MW, this difference
641 increased to ~10.5 times.

642 A similar trend was observed for peak sediment load, where the effect of cultivation at Area
643 C persisted at MW but was more pronounced. Under erosive cultivation, sediment load at MW
644 was ~23.5 times higher than under non-erosive conditions, compared to ~10.5 times at E2.
645 Additionally, peak sediment load at MW increased ~5.5 times relative to E2 under erosive
646 conditions, whereas for non-erosive cultivation, the increase was only ~1.5 times.

647 These findings suggest that, similar to peak flow, peak sediment load under non-erosive
648 conditions primarily originated from monitored overland flow at E2. However, during high-
649 energy runoff events, when severe erosion occurred, additional unmonitored sources—such
650 as tile drainage and diffuse overland flow—contributed significantly to sediment transport at
651 MW. Field evidence indicates that once a critical connectivity threshold was exceeded,
652 substantial overland flow bypassed the E2 monitoring point via alternative pathways that
653 connected directly to the stream at MW, amplifying turbidity and sediment load. This
654 observation aligns with threshold-driven hydrological connectivity in agricultural catchments,
655 where high flow conditions activate previously disconnected pathways, allowing unmonitored
656 sediment to reach downstream points like MW (Saffarpur et al., 2016).

657 Among unmonitored sediment sources, tile drainage systems—particularly Frau 1 and Frau
658 2—likely played a more significant role in sediment transport than previously assumed. These
659 systems provide an alternative sediment pathway, bypassing overland flow routes and
660 delivering fine sediments directly to the stream under specific hydrological conditions. Heavy
661 precipitation events, high antecedent soil moisture, and preferential flow through macropores
662 have been shown to trigger sediment-laden water transport via tile drains, circumventing
663 traditional overland flow pathways (King et al., 2015).

664 Unlike overland flow, which primarily transports coarser sediment fractions, tile drains
665 predominantly convey fine sediments, which can accumulate within the drainage pipes and



666 be intermittently flushed out during high-flow events. These sudden pulses of sediment
667 delivery are not necessarily linked to immediate overland flow, but rather occur when
668 hydrological connectivity between the fields and tile drains is established (Grangeon et al.,
669 2021; King et al., 2015). This intermittent flushing mechanism facilitates rapid and direct
670 sediment transfer to drainage outlets, thereby increasing sediment delivery to the stream
671 network (Grangeon et al., 2021). In some agricultural catchments, tile drains have been shown
672 to contribute to more than 50% of the annual sediment budget (Moore, 2016).

673 While tile drainage is unlikely to be the dominant sediment source in the HOAL catchment,
674 our findings suggest that it contributes more sediment than previously estimated. The tile
675 drains at Frau 1 and Frau 2 drain almost the entirety of Area C, representing a previously
676 unaccounted sediment transport pathway (Figure 3c,d). Additionally, the presence of mouse
677 holes in areas above the drainage system in Area C (Figure 11) suggests the formation of
678 preferential flow paths, which further enhance sediment transfer into tile drains. Such
679 preferential flow mechanisms accelerate sediment mobilization, allowing fine particles to
680 bypass natural retention and enter the stream unmonitored.



681

682 *Figure 11: Evidence of mouseholes above the tile drainage system in Area C. The images depict multiple small burrows created*
683 *by voles in grass-covered soil, forming macropores that enhance water and sediment infiltration. These macropores can serve*
684 *as preferential flow paths, facilitating rapid sediment transfer from agricultural topsoils into the tile drainage system,*
685 *particularly during high-flow events. This mechanism contributes to unmonitored sediment transport to drainage outlets,*
686 *reinforcing the role of subsurface connectivity in sediment mobilization. (Photos: BAW/Reinhard Hollerer)*

687 6. Conclusion

688 This study demonstrates that the effectiveness of non-erosive cultivation practices in reducing
689 turbidity and sediment load is highly dependent on topography, hydrological connectivity, and
690 field proximity to streams. Our findings at the hillslope scale (E2) indicate that non-erosive
691 cultivation significantly reduced peak turbidity (~9.5 times) and sediment load (~3.8 times) in
692 flat agricultural areas (<500 m from the stream, ~7.2% slope) but had no measurable effect in
693 steep (10–12% slope) or distant (>1000 m) agricultural fields, where high overland flow
694 velocities – driven by steeper topography – likely promote continued sediment detachment,
695 limiting the effectiveness of non-erosive cultivation in preventing soil erosion. Across all field
696 types, conversion to non-erosive cultivation had no significant effect on peak flow generation,



697 indicating that while these practices influence sediment transport, they do not regulate
698 overland flow volumes.

699 At the catchment scale (MW), dilution from subsurface flow reduced peak turbidity by 5.4–
700 7.7 times, whereas peak flow increased 2.8–11 times due to additional hydrological
701 contributions from wetlands, springs, and subsurface pathways. Peak sediment load at MW
702 was 2.4–5.4 times higher than at E2, suggesting that unmonitored diffuse overland flow and
703 tile drainage contribute to sediment mobilization at the catchment scale. These results
704 highlight the complexity of sediment connectivity in agricultural landscapes and the need for
705 multi-scale erosion control strategies.

706

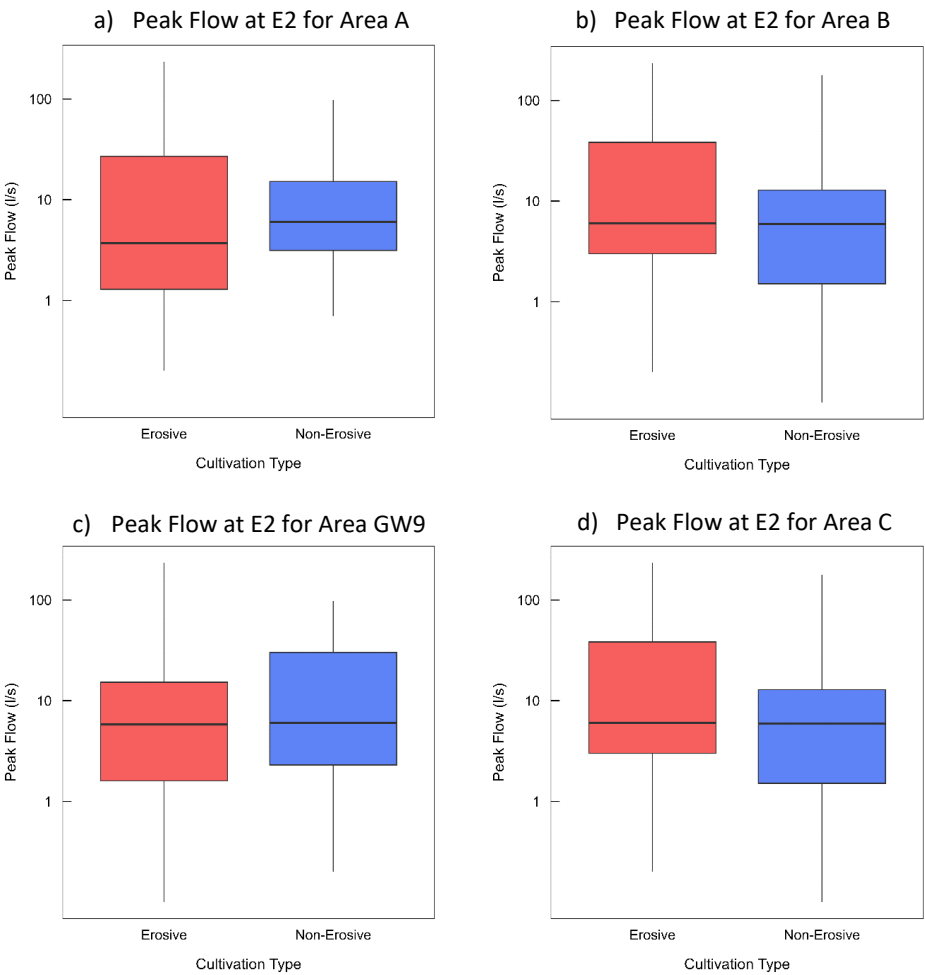
707



708 Appendix: Additional figures

709

710



711

712

713

714 **Figure A1:** Boxplots showing the distribution of peak flow (l/s) for different cultivation types
715 (erosive vs. non-erosive) at overland flow measurement site E2 in Areas a) A, b) B, c) GW9,
716 and d) C. The median, interquartile range, and outliers are displayed for each category. The y-
717 axis is on a logarithmic scale.

718

719

720

721

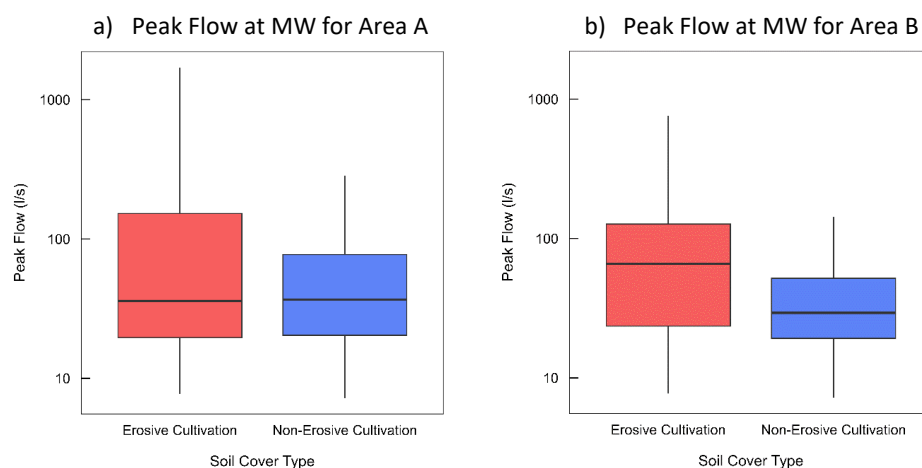
722

723



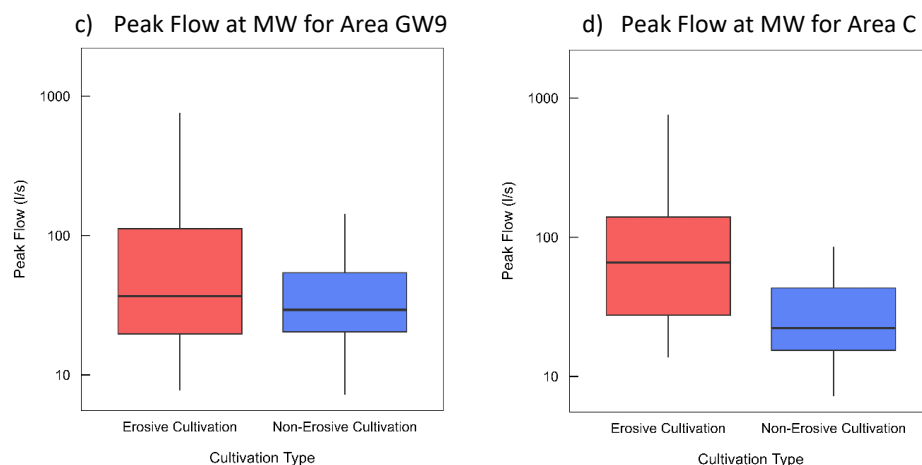
724

725



726

727



728

729 **Figure A2:** Boxplots showing the distribution of peak flow (l/s) for different cultivation types
 730 (erosive vs. non-erosive) at overland flow measurement site MW in Areas a) A, b) B, c) GW9,
 731 and d) C. The median, interquartile range, and outliers are displayed for each category. The y-
 732 axis is on a logarithmic scale.

733



734 References

- 735 Akinawo, S. O.: Eutrophication: Causes, consequences, physical, chemical and biological
736 techniques for mitigation strategies, *Environmental Challenges*, 12, 100733,
737 <https://doi.org/10.1016/j.envc.2023.100733>, 2023.
- 738 Arnold, J. G., Allen, P. M., Muttiah, R., and Bernhardt, G.: Automated base flow separation and
739 recession analysis techniques, *Groundwater*, 33, 1010–1018, <https://doi.org/10.1111/j.1745-6584.1995.tb00046.x>, 1995.
- 741 Basche, A. D., and DeLonge, M. S.: The impact of continuous living cover on soil hydrologic
742 properties: A meta-analysis, *Soil Science Society of America Journal*, 81, 1179–1190,
743 <https://doi.org/10.2136/sssaj2017.03.0077>, 2017.
- 744 Blann, K. L., Anderson, J. L., Sands, G. R., and Vondracek, B.: Effects of agricultural drainage on
745 aquatic ecosystems: A review, *Critical Reviews in Environmental Science and Technology*, 39,
746 909–1001, <https://doi.org/10.1080/10643380801977966>, 2009.
- 747 Blöschl, G., Blaschke, A. P., Broer, M., Bucher, C., Carr, G., Chen, X., Eder, A., Exner-Kittridge,
748 M., Farnleitner, A., Flores-Orozco, A., Haas, P., Hogan, P., Kazemi Amiri, A., Oismüller, M.,
749 Parajka, J., Silasari, R., Stadler, P., Strauss, P., Vreugdenhil, M., Wagner, W., and Zessner, M.:
750 The Hydrological Open Air Laboratory (HOAL) in Petzenkirchen: A hypothesis-driven
751 observatory, *Hydrology and Earth System Sciences*, 20, 227–255,
752 <https://doi.org/10.5194/hess-20-227-2016>, 2016.
- 753 Boardman, J., and Poesen, J.: Soil erosion in Europe: Major processes, causes, and
754 consequences, in: *Soil Erosion in Europe*, edited by: Boardman, J., and Poesen, J., Wiley,
755 Chichester, 477–487, <https://doi.org/10.1002/0470859202>, 2006.
- 756 Boix-Fayos, C., Barberá, G. G., López-Bermúdez, F., and Castillo, V. M.: Effects of check dams,
757 reforestation, and land-use changes on river channel morphology: Case study of the Rogativa
758 catchment (Murcia, Spain), *Geomorphology*, 91, 103–123,
759 <https://doi.org/10.1016/j.geomorph.2007.02.003>, 2007.
- 760 Borin, M., Vianello, M., Morari, F., and Zanin, G.: Effectiveness of buffer strips in removing
761 pollutants in runoff from a cultivated field in North-East Italy, *Agriculture, Ecosystems &
762 Environment*, 105, 101–114, <https://doi.org/10.1016/j.agee.2004.05.011>, 2005.
- 763 Borrelli, P., Robinson, D. A., Panagos, P., Lugato, E., Yang, J. E., Alewell, C., and Ballabio, C.:
764 Land use and climate change impacts on global soil erosion by water (2015–2070),
765 *Proceedings of the National Academy of Sciences*, 117, 21994–22001,
766 <https://doi.org/10.1073/pnas.2001403117>, 2020.
- 767 Bundesministerium für Land- und Forstwirtschaft, Regionen und Wasserwirtschaft (BML):
768 Evaluierung ÖPUL und Bodenerosion: Analyse der Wirkung von ÖPUL-Maßnahmen auf
769 Bodenerosionsschutz und Bodenfruchtbarkeit, <https://info.bml.gv.at/dam/jcr:579b01e2-745e-4f38-83ce-1f3c87244380/Evaluierung%20C3%96PUL%20und%20Bodenerosion.pdf>,
770 2021.



- 772 Chen, X., Parajka, J., Széles, B., Strauss, P., and Blöschl, G.: Spatial and temporal variability of
773 event runoff characteristics in a small agricultural catchment, *Hydrological Sciences Journal*,
774 65, 2185–2195, <https://doi.org/10.1080/02626667.2020.1798451>, 2020.
- 775 Doody, D. G., Archbold, M., Foy, R. H., and Flynn, R.: Approaches to the implementation of the
776 Water Framework Directive: Targeting mitigation measures at critical source areas of diffuse
777 phosphorus in Irish catchments, *Journal of Environmental Management*, 93, 225–234,
778 <https://doi.org/10.1016/j.jenvman.2011.09.002>, 2012.
- 779 Eder, A., Strauss, P., Krueger, T., and Quinton, J.: Comparative calculation of suspended
780 sediment loads with respect to hysteresis effects (in the Petzenkirchen catchment, Austria),
781 *Journal of Hydrology*, 389, 168–176, <https://doi.org/10.1016/j.jhydrol.2010.05.043>, 2010.
- 782 Eder, A., Exner-Kittridge, M., Strauss, P., and Blöschl, G.: Re-suspension of bed sediment in a
783 small stream: results from two flushing experiments, *Hydrology and Earth System Sciences*,
784 18, 1043–1052, <https://doi.org/10.5194/hess-18-1043-2014>, 2014.
- 785 Exner-Kittridge, M., Strauss, P., Blöschl, G., Eder, A., Saracevic, E., and Zessner, M.: The
786 seasonal dynamics of the stream sources and input flow paths of water and nitrogen of an
787 Austrian headwater agricultural catchment, *Science of The Total Environment*, 542, 935–945,
788 <https://doi.org/10.1016/j.scitotenv.2015.10.151>, 2016.
- 789 Firoozi, A. A., and Firoozi, A. A.: Water erosion processes: Mechanisms, impact, and
790 management strategies, *Results in Engineering*, 24, 103237,
791 <https://doi.org/10.1016/j.rineng.2024.103237>, 2024.
- 792 Food and Agriculture Organization (FAO): Soil erosion: The greatest challenge for sustainable
793 soil management, *FAO Soils Bulletin*, Rome,
794 <https://openknowledge.fao.org/handle/20.500.14283/ca4395en>, 2020.
- 795 Fryirs, K. A.: (Dis)Connectivity in catchment sediment cascades: A fresh look at the sediment
796 delivery problem, *Earth Surface Processes and Landforms*, 38, 30–46,
797 <https://doi.org/10.1002/esp.3242>, 2012.
- 798 Gentry, L. E., David, M. B., Royer, T. V., Mitchell, C. A., and Starks, K. M.: Phosphorus transport
799 pathways to streams in tile-drained agricultural watersheds, *Journal of Environmental Quality*,
800 36, 408–415, <https://doi.org/10.2134/jeq2006.0098>, 2007.
- 801 Giri, S., Qiu, Z., and Prato, T.: An integrated approach for targeting critical source areas to
802 control nonpoint source pollution in watersheds, *Water Resources Management*, 30, 5087–
803 5100, <https://doi.org/10.1007/s11269-016-1470-z>, 2016.
- 804 Grangeon, S., Ceriani, V., Evrard, O., Grison, A., Vandromme, R., Lefèvre, I., and Némery, J.:
805 Quantifying hydro-sedimentary transfers in a lowland tile-drained agricultural catchment,
806 *Catena*, 198, 105033, <https://doi.org/10.1016/j.catena.2020.105033>, 2021.



- 807 Gumiere, S. J., Le Bissonnais, Y., Raclot, D., and Cheviron, B.: Vegetated filter effects on
808 sedimentological connectivity of agricultural catchments in erosion modelling: A review, *Earth*
809 *Surface Processes and Landforms*, 36, 3–19, <https://doi.org/10.1002/esp.2042>, 2011.
- 810 Her, Y., Chaubey, I., and Frankenberger, J.: Effect of conservation practices implemented by
811 USDA programs at field and watershed scales, *Journal of Soil and Water Conservation*, 71,
812 249–266, <https://doi.org/10.2489/jswc.71.3.249>, 2015.
- 813 King, K. W., Williams, M. R., Macrae, M. L., Fausey, N. R., Frankenberger, J., Smith, D. R.,
814 Kleinman, P. J. A., and Brown, L. C.: Phosphorus transport in agricultural subsurface drainage:
815 A review, *Journal of Environmental Quality*, 44, 467–485,
816 <https://doi.org/10.2134/jeq2014.04.0163>, 2015.
- 817 Kirkby, M. J., Imeson, A. C., Bergkamp, G., and Cammeraat, L. H.: Scaling up processes and
818 models from the field plot to the watershed and regional areas, *Journal of Soil and Water*
819 *Conservation*, 51, 391–396, <https://doi.org/10.1080/00224561.1996.12457097>, 1996.
- 820 Kruskal, W. H., and Wallis, W. A.: Use of ranks in one-criterion variance analysis, *Journal of the*
821 *American Statistical Association*, 47, 583–621, <https://doi.org/10.2307/2280779>, 1952.
- 822 Lal, R.: Soil degradation by erosion, *Land Degradation & Development*, 12, 519–539,
823 <https://doi.org/10.1002/ldr.472>, 2001.
- 824 Lal, R.: Restoring soil quality to mitigate soil degradation, *Sustainability*, 7, 5875–5895,
825 <https://doi.org/10.3390/su7055875>, 2015.
- 826 Lin, Q., Xu, Q., Wu, F., and Li, T.: Effects of wheat in regulating runoff and sediment on different
827 slope gradients and under different rainfall intensities, *Catena*, 183, 104196,
828 <https://doi.org/10.1016/j.catena.2019.104196>, 2019.
- 829 Maetens, W., Poesen, J., and Vanmaercke, M.: How effective are soil conservation techniques
830 in reducing plot runoff and soil loss in Europe and the Mediterranean?, *Earth-Science Reviews*,
831 115, 21–36, <https://doi.org/10.1016/j.earscirev.2012.08.003>, 2012.
- 832 Montakhab, A., Yusuf, B., Ghazali, A. H., and Ghani, A. A.: Flow and sediment transport in
833 vegetated waterways: A review, *Reviews in Environmental Science and Biotechnology*, 11,
834 275–287, <https://doi.org/10.1007/s11157-012-9266-y>, 2012.
- 835 Montgomery, D. R.: Soil erosion and agricultural sustainability, *Proceedings of the National*
836 *Academy of Sciences*, 104, 13268–13272, <https://doi.org/10.1073/pnas.0611508104>, 2007.
- 837 Moore, J.: Literature review: Tile drainage and phosphorus losses from agricultural land, Lake
838 Champlain Basin Program Technical Report No. 83, 1–92, [https://www.lcbp.org/media-](https://www.lcbp.org/media-center/publications-library/publication-database/)
839 [center/publications-library/publication-database/](https://www.lcbp.org/media-center/publications-library/publication-database/), 2016. Nathan, R.J., and McMahon, T.A.
840 (1990). Evaluation of automated techniques for base flow and recession analyses. *Water*
841 *Resources Research*, 26(7), 1465–1473. <https://doi.org/10.1029/WR026i007p01465>



- 842 Nearing, M. A., Pruski, F. F., and O’Neal, M. R.: Expected climate change impacts on soil erosion
843 rates: A review: Conservation implications of climate change, *Journal of Soil and Water*
844 *Conservation*, 59, 43–50, <https://doi.org/10.1080/00224561.2004.12435709>, 2004.
- 845 Pastén-Zapata, E., Ledesma-Ruiz, R., Harter, T., Ramírez, A. I., and Mahlnecht, J.: Assessment
846 of sources and fate of nitrate in shallow groundwater of an agricultural area by using a multi-
847 tracer approach, *Science of the Total Environment*, 470–471, 855–864,
848 <https://doi.org/10.1016/j.scitotenv.2013.10.043>, 2014.
- 849 Pionke, H. B., Gburek, W. J., and Sharpley, A. N.: Critical source area controls on water quality
850 in an agricultural watershed located in the Chesapeake Bay Basin, *Ecological Engineering*, 14,
851 325–335, [https://doi.org/10.1016/S0925-8574\(99\)00059-2](https://doi.org/10.1016/S0925-8574(99)00059-2), 2000.
- 852 Reicosky, D. C.: Conservation tillage is not conservation agriculture, *Journal of Soil and Water*
853 *Conservation*, 70, 103A–108A, <https://doi.org/10.2489/jswc.70.5.103A>, 2015.
- 854 Rittenburg, R., Squires, A., Boll, J., Brooks, E., Easton, Z., and Steenhuis, T.: Agricultural BMP
855 effectiveness and dominant hydrological flow paths: Concepts and a review, *Journal of the*
856 *American Water Resources Association*, 51, 305–329, [https://doi.org/10.1111/1752-](https://doi.org/10.1111/1752-1688.12293)
857 1688.12293, 2015.
- 858 Sharpley, A. N., Gburek, W. J., Folmar, G., and Pionke, H. B.: Sources of phosphorus exported
859 from an agricultural watershed in Pennsylvania, *Agricultural Water Management*, 41, 77–89,
860 [https://doi.org/10.1016/S0378-3774\(99\)00018-9](https://doi.org/10.1016/S0378-3774(99)00018-9), 1999.
- 861 Skålevåg, A., Korup, O., and Bronstert, A.: Inferring sediment-discharge event types in an
862 Alpine catchment from sub-daily time series, *Hydrology and Earth System Sciences*, 28, 4771–
863 4796, <https://doi.org/10.5194/hess-28-4771-2024>, 2024.
- 864 Strauss, P., Leone, A., Ripa, M. N., Turpin, N., Lescot, J.-M., and Laplana, R.: Using critical source
865 areas for targeting cost-effective best management practices to mitigate phosphorus and
866 sediment transfer at the watershed scale, *Soil Use and Management*, 23, 144–153,
867 <https://doi.org/10.1111/j.1475-2743.2007.00118.x>, 2007.
- 868 Strauss, P., Schmaltz, E., Krammer, C., Zeiser, A., Weinberger, C., Kuderna, M., and Dersch, G.:
869 Bodenerosion in Österreich – Eine nationale Berechnung mit regionalen Daten und lokaler
870 Aussagekraft für ÖPUL: Endbericht, Bundesamt für Wasserwirtschaft, Institut für
871 Kulturtechnik und Bodenwasserhaushalt, Petzenkirchen, Austria,
872 [https://info.bml.gv.at/dam/jcr:cb1e8bdc-f2cf-4cb7-a229-](https://info.bml.gv.at/dam/jcr:cb1e8bdc-f2cf-4cb7-a229-02a30ef7037e/Bodenerosion%20in%20%C3%96sterreich_Endbericht.pdf)
873 02a30ef7037e/Bodenerosion%20in%20%C3%96sterreich_Endbericht.pdf, 2023.
- 874 Széles, B., Holko, L., Parajka, J., Stumpp, C., Stockinger, M., Komma, J., Rab, G., Wyhlidal, S.,
875 Schott, K., Hogan, P., Pavlin, L., Strauss, P., Schmaltz, E., and Blöschl, G.: Comparison of two
876 isotopic hydrograph separation methods in the Hydrological Open Air Laboratory, Austria,
877 *Hydrological Processes*, 38, e15222, <https://doi.org/10.1002/hyp.15222>, 2024.
- 878 Tomczak, M., and Tomczak, E.: The need to report effect size estimates revisited: An overview
879 of some recommended measures of effect size, *Trends in Sport Sciences*, 21, 19–25,
880 <https://doi.org/10.13140/RG.2.1.4620.0481>, 2014.



- 881 Tomer, M. D., and Schilling, K. E.: A simple approach to distinguish land-use and climate-
882 change effects on watershed hydrology, *Journal of Hydrology*, 376, 24–33,
883 <https://doi.org/10.1016/j.jhydrol.2009.07.029>, 2009.
- 884 U.S. Environmental Protection Agency: Connectivity of streams and wetlands to downstream
885 waters: A review and synthesis of the scientific evidence (EPA/600/R-14/475F), Office of
886 Research and Development, U.S. Environmental Protection Agency, Washington, DC,
887 <https://cfpub.epa.gov/ncea/risk/recorddisplay.cfm?deid=296414>, 2015.
- 888 Van Oost, K., Quine, T. A., Govers, G., De Gryze, S., Six, J., Harden, J. W., Ritchie, J. C., McCarty,
889 G. W., Heckrath, G., Kosmas, C., Giraldez, J. V., da Silva, J. R. M., and Merckx, R.: The impact of
890 agricultural soil erosion on the global carbon cycle, *Science*, 318, 626–629,
891 <https://doi.org/10.1126/science.1145724>, 2007.
- 892 Vercruysse, K., Grabowski, R. C., and Rickson, R. J.: Suspended sediment transport dynamics
893 in rivers: Multi-scale drivers of temporal variation, *Earth-Science Reviews*, 166, 38–52,
894 <https://doi.org/10.1016/j.earscirev.2016.12.016>, 2017.
- 895 Verstraeten, G., Van Oost, K., Van Rompaey, A., Poesen, J., and Govers, G.: Evaluating an
896 integrated approach to catchment management to reduce soil loss and sediment pollution
897 through modelling, *Soil Use and Management*, 18, 386–394, [https://doi.org/10.1111/j.1475-](https://doi.org/10.1111/j.1475-2743.2002.tb00257.x)
898 2743.2002.tb00257.x, 2002.
- 899 Wischmeier, W. H., and Smith, D. D.: Predicting rainfall erosion losses—A guide to
900 conservation planning (Agriculture Handbook No. 537), U.S. Department of Agriculture,
901 Science and Education Administration, 1978.
- 902 Wu, L., Peng, M., Qiao, S., and Ma, X.: Effects of rainfall intensity and slope gradient on runoff
903 and sediment yield characteristics of bare loess soil, *Environmental Science and Pollution*
904 *Research*, 25, 3480–3487, <https://doi.org/10.1007/s11356-017-0713-8>, 2018.
- 905 Zhang, X. C., Zheng, F. L., Chen, J., and Garbrecht, J. D.: Characterizing detachment and
906 transport processes of interrill soil erosion, *Geoderma*, 376, 114549,
907 <https://doi.org/10.1016/j.geoderma.2020.114549>, 2020.
- 908



909 [Code availability](#)

910 The pieces of code that were used for all analyses are available from the authors upon request.

911 [Data availability](#)

912 The datasets that have been analysed in this paper are available from the authors upon
913 request.

914 [Author contribution](#)

915 CT: Conceptualization, Data Curation, Formal Analysis, Investigation, Methodology, Software,
916 Visualization, Writing (original draft preparation), Writing (review and editing)

917 BS: Data Curation, Conceptualization, Methodology, Writing (review and editing)

918 MB: Data Curation, Methodology, Writing (review and editing)

919 ES: Data Curation, Resources, Writing (review and editing)

920 CK: Data Curation, Resources, Writing (review and editing)

921 PS: Funding acquisition, Project administration, Supervision, Writing (review and editing)

922 GB: Funding acquisition, Project administration, Supervision, Writing (review and editing)

923 [Competing interests](#)

924 At least one of the (co-)authors is a member of the editorial board of *Hydrology and Earth*
925 *System Sciences*.